Chapter 2
Stratigraphy and Sedimentology of Azokh Caves, South Caucasus

John Murray, Edward P. Lynch, Patricio Domínguez-Alonso, and Milo Barham

Abstract The Pleistocene to Holocene stratigraphy of sediments from three entrance passages to Azokh Cave, Lesser Caucasus, is presented. The larger Azokh 1 passage preserves approximately 11–12 m of *in situ* cave-fill, divisible into nine stratigraphic units based on their sedimentary characteristics. The base of the succession (Units IX to VI) is predominantly non-fossiliferous, but becomes both fossiliferous and calcareous upwards and displays evidence of fluvial and cave spall deposition. The upper part of the succession (Units V to I) is a (largely) continuous sequence of generally fossiliferous fine-grained sediments dating from the Middle Pleistocene to the present. The Pleistocene-Holocene transition is not represented in the succession due to a marked erosional disconformity between Units II and I (at the top of the sequence). The entrance passage to Azokh 2 contains a fill of at least 1.65 m depth that is divisible into two distinct units, whilst the interior of Azokh 5 has revealed at least 4.5 m of cave-filling sediment, which is divisible into five stratigraphic units (A–E). Unit A, at the top of the Azokh 5 sequence, has produced charcoal which provided an age of 2.3 ka and sits with marked discontinuity on the irregular upper surface of Unit B below. The ages of the units beneath this level are unknown at present.

Резюме Пещерная сеть Азоха образовалась в мезозойском известняке. Значительные объемы отложений были выявлены в трех из ее входных коридоров. Стратиграфия коридора *Азох 1* наиболее полно изучена среди трех обнаруженных входов; он раскапывается с 1960-х гг. и охватывает примерно 11–12-метровый слой седимента, датирующегося от по меньшей мере среднего плейстоцена (и, возможно, еще древнее) до настоящего времени. Переход между плейстоценом и голоценом визуально не обнаруживается по причине выраженного эрозионного несоответствия в седиментной последовательности по направлению к вершине.

Нижерасположенная в *Азох 1* и находящаяся близко с выходу субкамера вмещает в себя то, что получило название *седиментная последовательность 1*. Ее почти 4,5-метровой толщины срез включает подразделения *IX–VI* (в восходящем стратиграфическом порядке) и, за исключением самого верхнего слоя, вероятнее всего, преимущественно не содержит окаменелостей. Предшествующее палеомагнетическое исследование подсказало, что основание последовательности фактически может быть раннеплейстоценовым (калабрийским) по возрасту. *Седиментная последовательность 2* расположена далее вовнутрь от выхода в *Азох 1* и в значительной степени залегает над *седиментной последовательностью 1*. Эта около 8,5-метровой толщины последовательность разделяется на пять подразделений (*V–I*). Подразделения *V–II* содержат богатую и разнообразную средне- и верхнеплейстоценовую фауну. Свидетельства человеческой активности (в форме каменных орудий и следов разреза на костях) также были найдены в этих слоях. Среднеплейстоценовый (пренеандертальский) фрагмент нижней челюсти человека был обнаружен примерно на уровне подразделения *V*, хотя

Patricio Domínguez-Alonso – Deceased

J. Murray (✉) · E.P. Lynch · M. Barham
Earth & Ocean Sciences, School of Natural Sciences,
National University of Ireland, Galway,
University Road, Galway, Ireland
e-mail: john.murray@nuigalway.ie

E.P. Lynch
e-mail: edward.lynch@nuigalway.ie

Present Address:
M. Barham
Department of Applied Geology, Curtin University,
GPO Box U1987, Perth, WA 6845, Australia
e-mail: milobarham@yahoo.co.uk

P. Domínguez-Alonso
Departamento de Paleontología, Facultad de Ciencias Geologicas
& Instituto de Geociencias (IGEO-CSIC), Universidad
Complutense de Madrid (UCM), Madrid, Spain

Yolanda Fernández-Jalvo et al. (eds.), *Azokh Cave and the Transcaucasian Corridor*,
Vertebrate Paleobiology and Paleoanthropology, DOI 10.1007/978-3-319-24924-7_2

его точная датировка неизвестна. Седиментное наполнение коридора *Азох 1* преимущественно мелкозернистое, свидетельствуя или о низкоэнергетическом водном потоке (возможно, вследствие запруживания как результата затопления внутреннего сегмента пещерной системы), или, вероятно, из-за изменения его направления по причине сильных ветров. Обнаружены также горизонты, содержащие скопления осколков крупнозернистого известняка. Их значение непонятно, однако они могут указывать на изменения в палеоэкологических условиях, такие как рост просачивания воды через пещеру или заметное похолодание климата. Влияние геоморфологических и тектонических факторов, как, например, увеличение сейсмической активности, также нельзя не принимать в расчет.

Меньший по размерам коридор *Азох 2* расположен примерно в 42 м на северо-восток от коридора *Азох 1*. К настоящему времени полностью идентифицируемыми в отношении наполнителей являются два стратиграфически подразделения. Самое верхнее из них (подразделение *1*) содержит различные слои очагов, в одном из которых был найден скелет человека, датированный периодом голоцена. Лежащее ниже подразделение *2* заметно светлее по окраске и более кальцифицировано. Его общая толщина пока не выяснена и, поскольку в нем не обнаружено никаких окаменелостей или артефактов, возраст данного подразделения остается неизвестным.

На расстоянии около 100 м от *Азох 1* находится коридор *Азох 5*. Это маленькая фреатическая труба, которя ведет к внутренней камере, с седиментным покрытием толщиной, по меньшей мере, 4,5 м. Данная величина, вероятнее всего, значительно занижена, поскольку вершина и основание последовательности слоев не были визуально идентифицированы, а геофизики оценили общую толщину седиментного наполнения около 10 м. К настоящему времени идентифицированы пять подразделений (помеченных как *A–E* в стратиграфически нисходящем порядке). Седиментные слои обычно мелкозернистые, хотя подразделения *D* и *B* характеризуются повышенным содержанием крупнозернистого известняка и обломков кремня, большинство из которых имеет местное происхождение. Обратное соотношение было обнаружено между подразделениями *B* и *A* на самой вершине седиментного покрытия. В подразделении *A* найден древесный уголь, датируемый 2300 г. до н.э., однако возраст подразделения под находками до сих пор остается неизвестным.

Keywords Azokh Cave • Lesser Caucasus • Stratigraphy • Middle Pleistocene • Sediment

Introduction

Cave systems are a typical feature of karst landscapes where they develop through the dissolution of soluble bedrock, leading to the formation of a variety of open-space cavities and passageways. They represent a geomorphologic link between the surface and sub-surface environments, provide a conduit for the flow of groundwater and act as a natural repository for the accumulation of sediment (e.g., Bogli 1980; White 1988; Sasowsky and Mylroie 2004). Caves also act as natural shelters for animals and have been similarly exploited for thousands of years by humans. Consequently, caves and rock shelters represent a habitat that may have assisted in the intellectual development of human kind (e.g., Chauvet et al. 1996).

In recent years, investigations into the geological, hydrogeological and biogeochemical properties of cave systems have transformed our understanding of cave genesis (Moore and Sullivan 1997; Engel et al. 2004; Ford and Williams 2007). In particular, studies of cave-fill sediments have provided new insights into the timing of cave formation, subterranean environmental processes, karst landscape evolution, groundwater dynamics and paleoclimatology (e.g., Bretz 1942; Polyak et al. 1998; Musgrave and Webb 2004; Pickering et al. 2007; White 2007). Thus, the study of cave sediments can increase our understanding of the sedimentological and environmental conditions that existed during the formation and evolution of a cave system. In addition, cave sediment deposits are frequently associated with fossil preservation and have proven to be important sites for the discovery of archaeological artifacts and hominin remains (Jelinek 1982; Torres et al. 2003; Pinhasi et al. 2008; Dirks et al. 2010; Moldovan et al. 2011; Pickering et al. 2011).

This chapter reviews the stratigraphic and sedimentary characteristics of Azokh Cave, with particular emphasis on its three main entrance passages: Azokh 1, Azokh 2 and Azokh 5. We summarize the nature of cave-fill sediments within Azokh 1 passage, as previously reported by Murray et al. (2010), and provide additional data (sedimentological, textural, mineralogical) that further constrain the stratigraphy. Azokh 1 has been the principal site of archaeological excavation at the cave since 2002 (Fernández-Jalvo et al. 2009, 2016). In addition, an assessment of the stratigraphy and sedimentology of Azokh 2 and Azokh 5 entrance passages is also made. Knowledge of the sedimentary infill within these smaller passageways is presently at a reconnaissance level and the data presented herein should thus be viewed as preliminary.

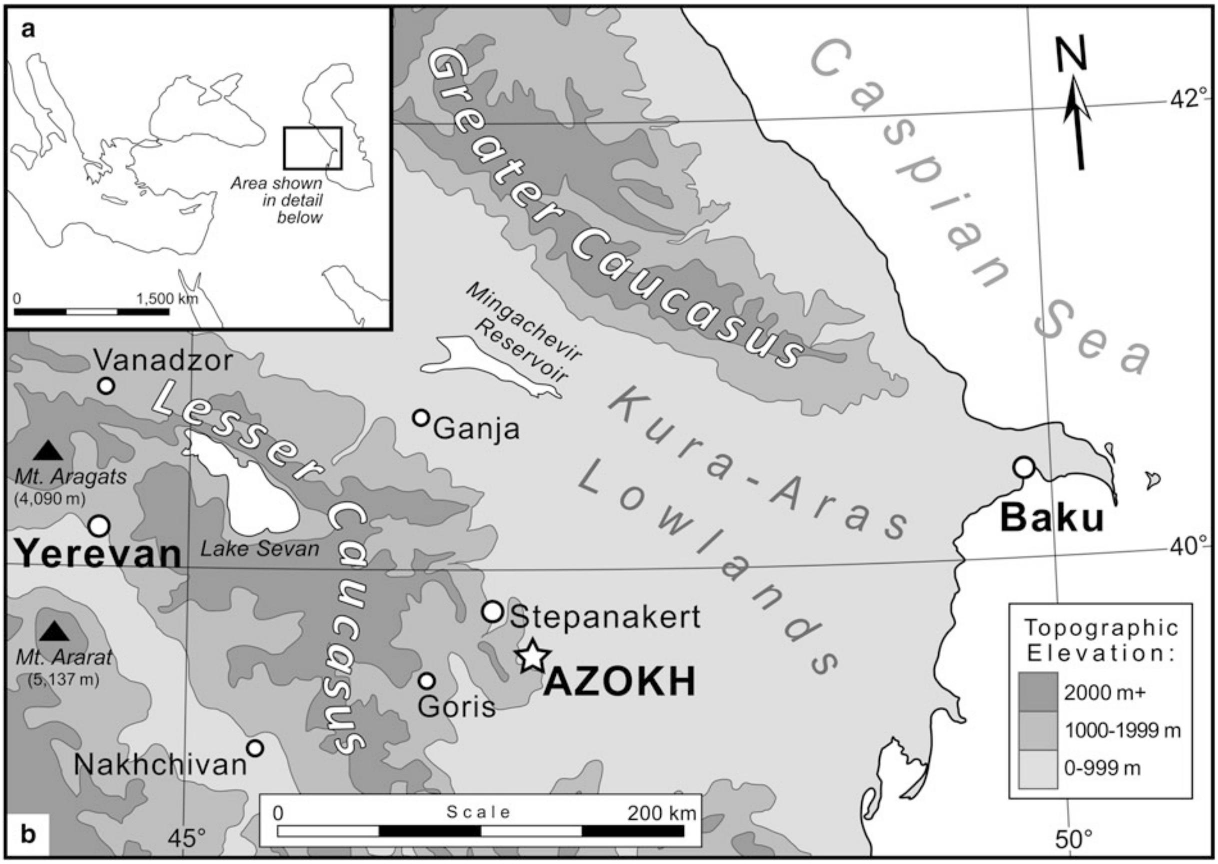

Fig. 2.1 Geographic location of Azokh Cave in the South Caucasus. **a** General view of region relative to the Eastern Mediterranean, Black and Caspian seas. **b** More detailed view of location, with an indication of topographic elevation shown. Position of (**b**) is indicated by inset box in (**a**)

Geological Setting and Overview of the Azokh Cave System

Azokh Cave (located at 39º 37.15′ north; 46º 59.32′ east; Fig. 2.1) is hosted in a thickly-bedded sequence of Mesozoic (possibly Jurassic) limestone that has experienced variable levels of uplift and karstification since the Pleistocene (Lioubine 2002). The carbonate bedrock forms part of a limestone massif that is developed on a regional-scale across the Southern Caucasus (Khain 1997). In the vicinity of the cave, the host limestone is a fossiliferous grainstone which has undergone partial silicification, possibly due to the combined input of volcanogenic siliciclastics and siliceous fossil material. The cave system comprises a series of dissolution cavities that may have developed partly in response to vadose zone fluviokarst processes (e.g., White 1988; Domínguez-Alonso et al. 2016). The cave consists of a NNW- to SSE-aligned internal zone that is composed of several interconnected, sub-rounded chambers extending over approximately 130 m (Fig. 2.2). This main body of the cave is transected on its western flank by several WSW- to ENE-trending entrance passageways that connect the internal zone to the exterior (Figs. 2.2 and 2.3). The orientation of the main chamber and entrance passages broadly corresponds with the alignment of conjugate joint sets and fractures that are pervasively developed in the limestone bedrock (Domínguez-Alonso et al. 2016).

The initial investigations of Azokh Cave by the Huseinov team in the 1960s did not establish a clear and detailed record of the Pleistocene and Holocene sedimentary infill of the cave system (Mustafayev 1996; Lioubine 2002). In particular, early excavations lacked any rigorous stratigraphic control. Sedimentary units were more commonly distinguished based on their archaeological content, rather than their sedimentological properties (Lioubine 2002). Definitive thickness estimates for the sedimentary units identified at that time appear not to have been unequivocally

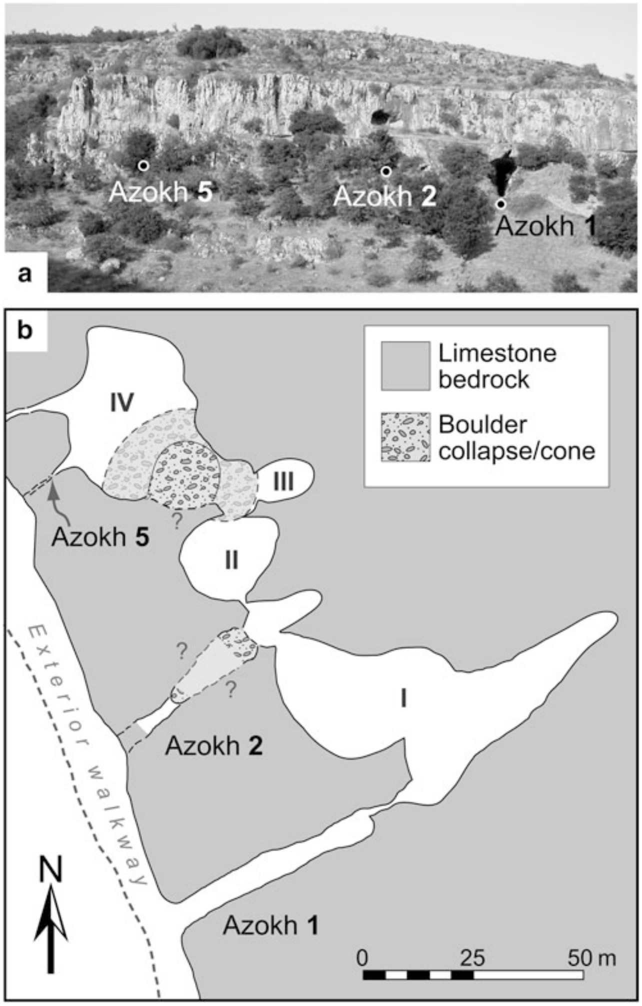

Fig. 2.2 **a** Field photograph of the west-facing hillside containing the Azokh Cave system. Locations of Azokh 1, 2 and 5 entrance passages are indicated. **b** Simplified plan-view sketch map of the cave system showing the location of the main entrance passages. Internal cave chambers are labeled with roman numerals (I–IV). Reproduced from Murray et al. (2010)

established and any lateral shifts in sedimentary facies were not made apparent. In addition, systematic archaeological excavation methods, utilizing aerial grids and three-dimensional spatial recording of finds, were not employed. These factors have combined to make the understanding of the context and significance of the large volume of fossil and lithic artifacts recovered prior to 2002 a challenging prospect.

Azokh 1

The Azokh 1 passageway is a broadly linear chamber measuring 40 m long by 11.5 m high with a WSW-ENE alignment (Fig. 2.4). This orientation results in the entranceway being well illuminated, particularly by the afternoon sun. Towards the interior of the passage, in an ENE direction ("Uppermost Platform" in Fig. 2.4), the light is not as good and artificial illumination has been employed there during excavation work. The floor of the chamber drops (slopes) down at approximately the midway point in the passage, which increases the height of the chamber to approximately 14 m towards the entrance. The sedimentary infill of Azokh 1 passage yielded a human jaw fragment in 1968 that was later assessed as Middle Pleistocene in age (Kasimova 2001). The nature of this discovery in the southern Caucasus (Fig. 2.1), coupled with additional archaeological and paleontological finds, has established Azokh 1 as a site of significant archaeological and paleoanthropological interest (e.g., Ljubin and Bosinski 1995; Bridgland et al. 2006; Fernández-Jalvo et al. 2010; Pinhasi et al. 2011).

During these early phases of excavation, a considerable amount of sediment was removed from the passageway (Fig. 2.3a), and Lioubine (2002) noted that before the first excavations in the 1960s, the chamber was filled to within 2–3 m of the roof. A graphical estimate of the original sediment thickness is provided in Figs. 2.3a and 2.4 and it is apparent that a considerable amount of the stratigraphic section is now gone. Huseinov initially identified 10 stratigraphic horizons infilling the chamber during the 1960s. This was increased to 17 by Veilicko in 1979 and then to 25 by the Gadzhiev team in 1980 (Huseinov 1985; Lioubine 2002). Detailed records of the extent of these excavations and the amount of sediment removed are no longer readily available. Therefore, an appraisal of the sedimentology incorporating the full pre-2002 stratigraphic sequence is extremely difficult to ascertain. In this regard, what is presented below is a description based on the stratigraphic remnants that we found remaining in the passage.

When excavation work restarted in 2002, the Azokh 1 passageway was an obvious priority for renewed investigation and was initially termed *Azokh Main*. Subsequently, the passage was renamed *Azokh 1* following reconnaissance geophysics and geological work that identified appreciable thicknesses of sediment fill in two other entrance

Fig. 2.3 Field photographs of entrance passages to Azokh Cave. **a** Azokh 1. The distinctive sediment pedestal marking the entranceway is visible towards the bottom of the image. The white asterisk indicates the approximate position of the original sediment infill of the passage, prior to excavation in the 1960s and 70s. **b** Azokh 2 and **c** Azokh 5. Both (**b**) and (**c**) were photographed in 2004. The hammer for scale (highlighted with a white arrow in both images) is 35 cm long

passageways – Azokh 2 and Azokh 5 (Fig. 2.3b, c; see also Fig. 2.2 for general location). Post-2002, systematic and detailed archaeological investigations have been conducted in the upper half of the sedimentary sequence remaining in Azokh 1 (Asryan et al. 2016; Fernández-Jalvo et al. 2016; King et al. 2016).

The most recent assessment of the stratigraphy of Azokh 1 was provided by Murray et al. (2010) and their proposed lithostratigraphic framework is retained here. Nine sedimentary units, occurring within two physically separated stratigraphic remnants (termed Sediment Sequences – see Fig. 2.4), are recognized based on their sedimentological properties. Sediment Sequence 1 is located at the ENE end of a basal trench at the cave entrance and accounts for 4.5 m of stratigraphy (Fig. 2.5). Sediment Sequence 2 is located towards the rear of Azokh 1 passage and is estimated to be at least 8.5 m thick (Fig. 2.6). This latter sequence is interpreted to have overlain the former, although since no physical connection remains between the two sequences, and practically no sediments remain along the sides of the cave walls, this inference is equivocal.

Table 2.1 summarizes the main stratigraphic subdivisions of the infill of Azokh 1. It provides average estimates of the color, texture and sedimentary characteristics of the various lithostratigraphic units and is built upon the descriptions presented in Murray et al. (2010). Detailed excavation work, particularly towards the top of the stratigraphic succession, has revealed much intra-unit variation. This has become particularly evident as horizons have been tracked laterally from the center of the passageway, where most of the lithostratigraphic units were originally diagnosed, and out towards the cave walls.

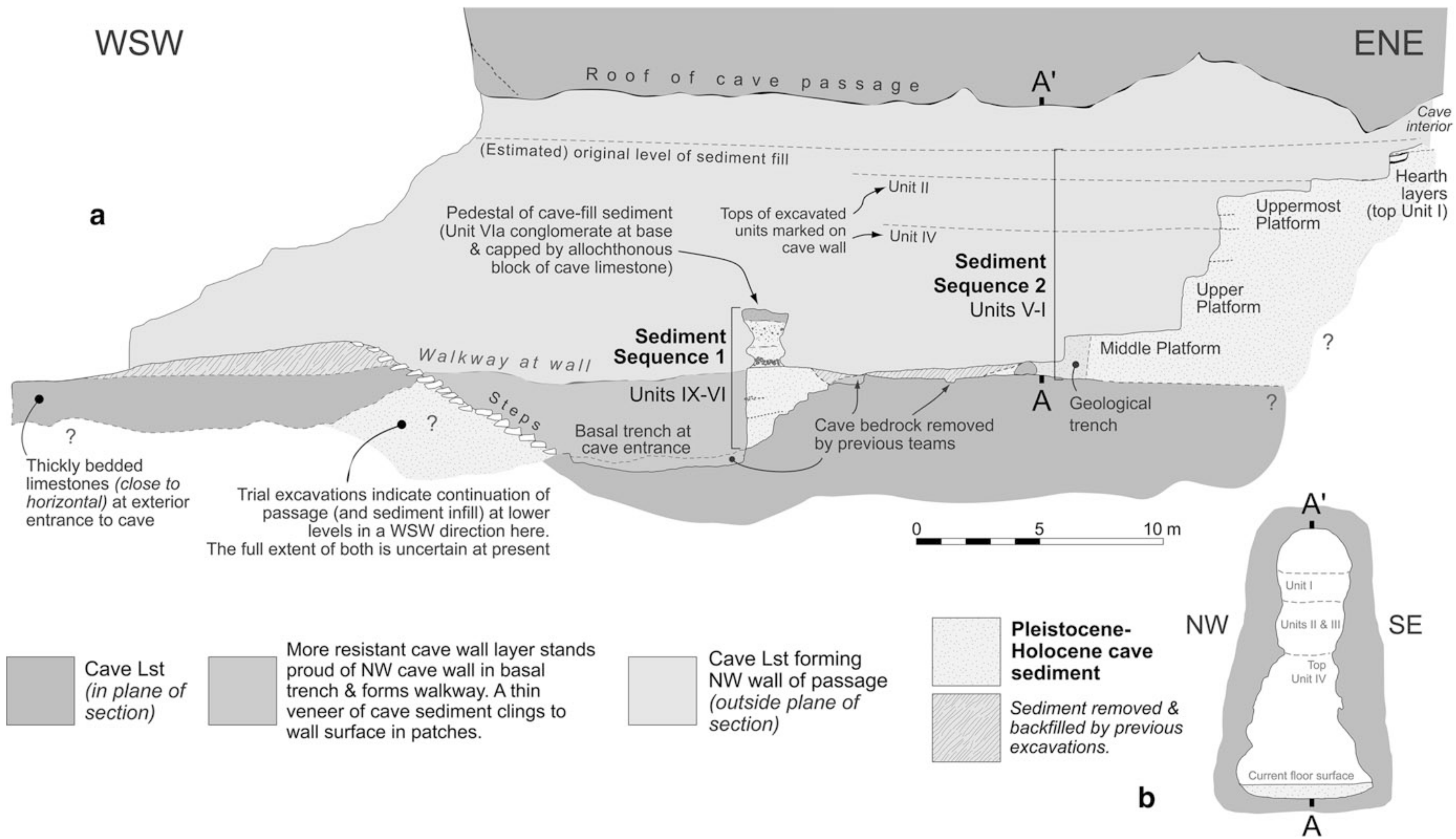

Fig. 2.4 **a** Sketch cross-section through Azokh 1 cave passage (drawn facing NW). The estimated amount of cave-fill sediment removed by previous excavation teams is indicated by the upper dashed line. The floor of the passage is illustrated insofar as its extent is currently known and the height of the roof was measured at various points along the section using a telemeter with an accuracy of 1 cm. **b** Cross-section (A–A′) across the axis of the passage [orthogonal to (**a**) and drawn to the same scale] indicates levels of sediment infill. Reproduced from Murray et al. (2010)

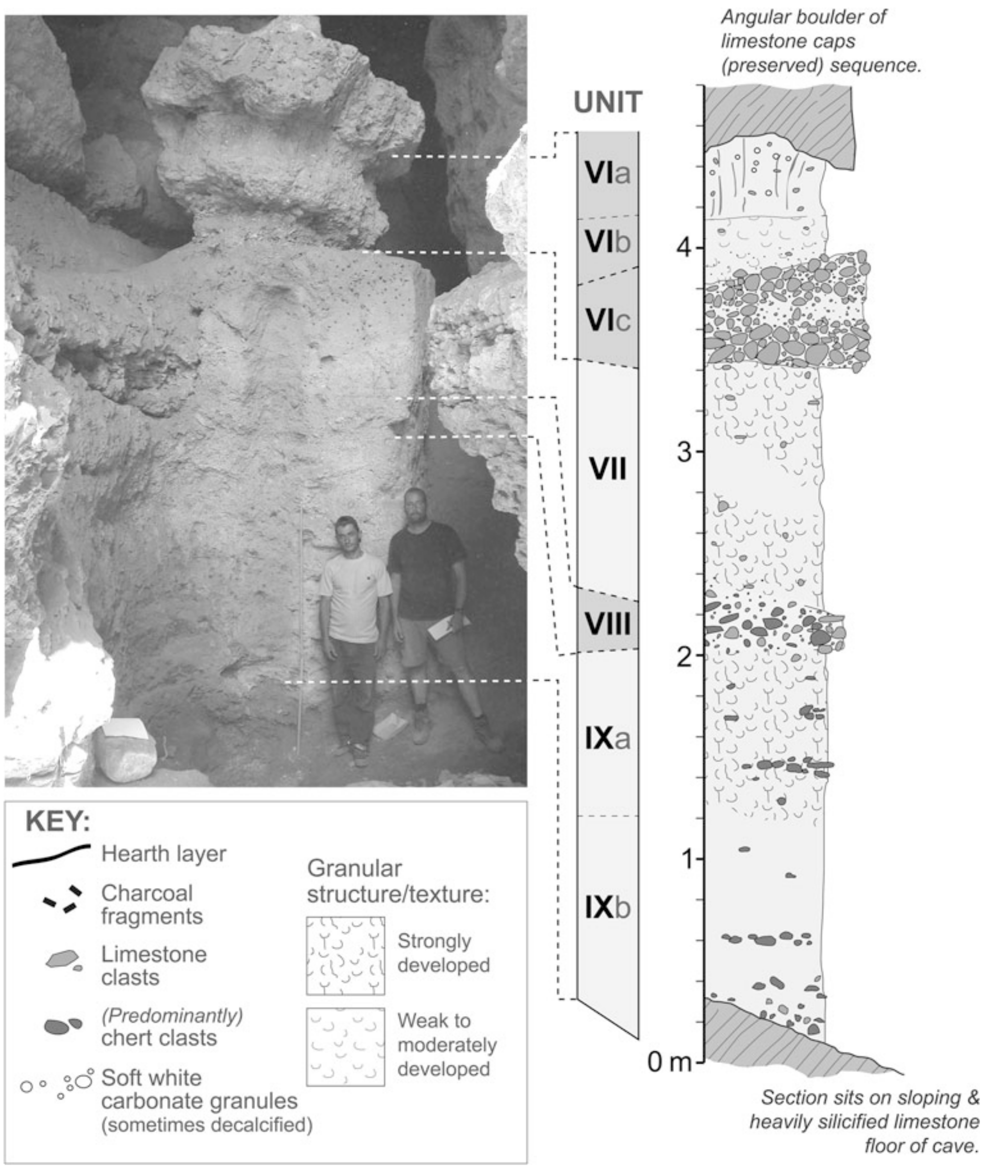

Fig. 2.5 Stratigraphic column for Sediment Sequence 1 in Azokh 1 passage. Unit numbers are indicated in the central column with roman numerals. The photograph of the actual section to the left of the column is for reference and indicates precisely where the boundaries of the units have been set. Much of this section is exposed in the basal trench in the entrance to the cave (see Fig. 2.4). The key to the various sedimentological features is also applicable to Fig. 2.6. Reproduced from Murray et al. (2010)

Sediment Sequence 1

This sequence occupies a lower sub-level within Azokh 1 passage (Fig. 2.4) and it contains Units IX to VI (Fig. 2.5). Given that it rests on a down-sloping cave floor surface (Fig. 2.7; see also Fig. 2.4), the section effectively wedges out, so the amount of remaining stratigraphy becomes progressively more limited moving downwards. The base of the sequence (Units IX and VIII) is largely composed of non-calcareous sandy loam/loamy sand (Table 2.1). A gradual and pronounced development of a granular structure midway through Unit IX (Fig. 2.8) marks the contact between its two constituent subunits. The overlying Unit VIII is characterized by a higher concentration of limestone and chert clasts. The contacts of Unit VIII with its bounding (enclosing) units are not sharply defined and it is possible that it may represent a localized accumulation of larger clast types within a loamy sand matrix.

Units VII and VI above see a shift to clay-loam textures, with the exception of subunit VIc which is a conspicuous clast-supported pebble to cobble conglomerate (Fig. 2.9). The two subunits (VIb and VIa) overlying the conglomerate are calcareous, and this contrasts with the non-calcareous units beneath. Sediment Sequence 1 is capped by a large

Table 2.1 Stratigraphic divisions and character of the remaining sediments in Azokh 1

	Unit/ Sub-unit		Thickness	Consistence & Texture	Structure	Color (Munsell)	Rocks/clasts/comments	Carbonates	Age	
Sediment Sequence 2 (Units V–I)	I		80–150 cm	Generally friable to loose clay loam	Moderate granular	7.5YR 4.5/3 (Brown)	Limestone clasts are rare and are often strongly altered. This unit contains the very distinctive fumier near the top	Non-calcareous	157 ± 26 years BP	Holocene
	II		c. 101–140 cm (Minimum – unit appears to thicken towards cave interior)	Quite variable (vertically & laterally), but generally [sandy] clay loam. Base is firm becoming friable-firm upwards	Moderate granular at base, granular at top	10YR 5/3 (Brown)	Pebble-grade limestone clasts (0.5–5 cm) are present and commonly decalcified and/or altered. Small white carbonate granules dispersed throughout. Disseminated charcoal fragments noted in the top 30 cm. Bone fragments are common and are often poorly preserved. The top of this unit is quite irregular and accounts for much of the thickness variation	Base is calcareous; however, top is non-calcareous, particularly in center of cave passage	*Top:* 100 ± 7 ka *Base:* 184 ± 13 ka	Late Pleistocene
	III		60–70 cm	Friable clay to silty clay	Top half is weak to moderate granular. Bottom half is very weak granular (almost massive)	10YR 4.5/4.5 (Dark yellowish brown)	Limestone clasts are reduced in size and concentration; however, fragments up to 18 cm noted. Bone and charcoal are also present. The contact with Unit IV below is indistinct in places, particularly when traced out laterally towards the cave walls	Very strongly calcareous	–	Middle Pleistocene (Units V–III)
	IV		100–122 cm	Friable silty clay	Weak fine granular at base, becoming moderate medium granular upwards	10YR 5/4 (Yellowish-brown)	Limestone clasts are dispersed and uncommon in the base. Flattened sub-angular to rounded limestone pebble and cobble clasts become more common towards the top of the unit. Bone and charcoal are present	Weakly calcareous	Units V–IV (contact): 205 ± 16 ka	
	V	Va	220–230 cm	Predominantly friable silty clay	Variable, but generally massive with a granular base	Variable between 10YR 5/5 (Yellowish brown) at base and 7.5YR 4.5/5 (Brown) above	2–10 mm flattened angular limestone clasts are common in basal c. 55 cm. The overlying c. 105 cm has dispersed sand-grade material in lower 2/3^{rds} followed by horizontal flattened limestone clasts. The contact between Va and Vb is marked in places by a thin, yet conspicuous cream-white to white non-calcareous crust	Calcareous		
		Vb	220–230 cm	Variable between friable-firm loamy sand (particularly near base) and friable clay loam	Variable, but generally massive	10YR 6/3 (Pale brown) at base, 7.5YR 4/4 (Brown) above	This unit is best exposed in a geological trench (see Figs. 2.4 and 2.10). Contains rare limestone clasts, but lensoidal "channel" structures contain elevated concentrations of clasts	Largely non-calcareous	293 ± 23 ka	

(continued)

Table 2.1 (continued)

	Unit/	Sub-unit	Thickness	Consistence & Texture	Structure	Color (Munsell)	Rocks/clasts/comments	Carbonates	Age
Sediment Sequence 1 (Units VI–IX)	VI	VIa	10–40 cm	Soft friable clay/clay loam	Moderate granular with an additional prismatic component	7.5YR 5/4 (Brown)	The variation in the thickness of this subunit reflects the irregularity of the base of a large angular limestone boulder which caps the preserved sequence. Abundant mm-scale white carbonate clasts are present along with bone and charcoal	Strongly calcareous	**Sequence 1 is undated** Previous paleomagnetic work reported by Huseinov (1985) and also Ljubin and Bosinski (1995) suggest lower part of this sequence is Early Pleistocene in age (Units IX–VI)
		VIb	30–33 cm	Very firm to firm sandy clay loam	Weakly developed fine to medium granular	7.5YR 4/4 (Brown)	Rounded and angular pebble and granule-grade clasts occur throughout. Flattened and degraded white carbonate clasts are common in parts of the base. Bone fragments present, but uncommon	Calcareous	
		VIc	30–60 cm	*Friable to loose clast-supported conglomeratic marker horizon*			Fossil bone fragments noted in the base of this conspicuous subunit	Conglomerate clasts react with HCl	
	VII		110–115 cm	Friable to firm clay loam	Granular top (30–50 cm) and base (48–60 cm) Midsection is massive	10YR 5.5/3.5 (Brown to yellowish brown)	Gravel to small pebble-grade chert and decalcified limestone clasts are dispersed throughout; however, they are rare in the midsection of the unit. The contact with underlying Unit VIII is gradational and is marked by a conspicuous drop in clast content	Non-calcareous	
	VIII		20–30 cm	Firm loamy sand	Medium granular	10YR 6/4 (Light yellowish brown)	Poorly-sorted (largely) matrix-supported conglomerate. Clasts are generally sub- to well-rounded cherts and decalcified limestones and range in size from gravel to cobble grade. This appears to be quite a localised feature	Non-calcareous	
	IX	IXa	70–85 cm	Firm loamy sand to sandy loam	Strongly medium to coarse granular	10YR 6.5/3 (Pale to light yellowish brown)	Contains a matrix-supported population of sub-rounded to angular limestone and chert clasts ranging 2–6 cm. Granular texture is main distinguishing feature from subunit IXb below and it develops over a c. 15 cm stratigraphic interval	Non-calcareous	
		IXb	110–125 cm	Firm to very firm sandy loam	Massive	10YR 6/4 (Light yellowish brown)	This subunit drapes the irregular topography of the cave floor. Dispersed granules of cave rock, some concentrated in poorly defined bedding-parallel seams/pockets, are present in the basal c. 60 cm. Rare clasts noted in the top 60 cm, which is more uniform in character	Non-calcareous	

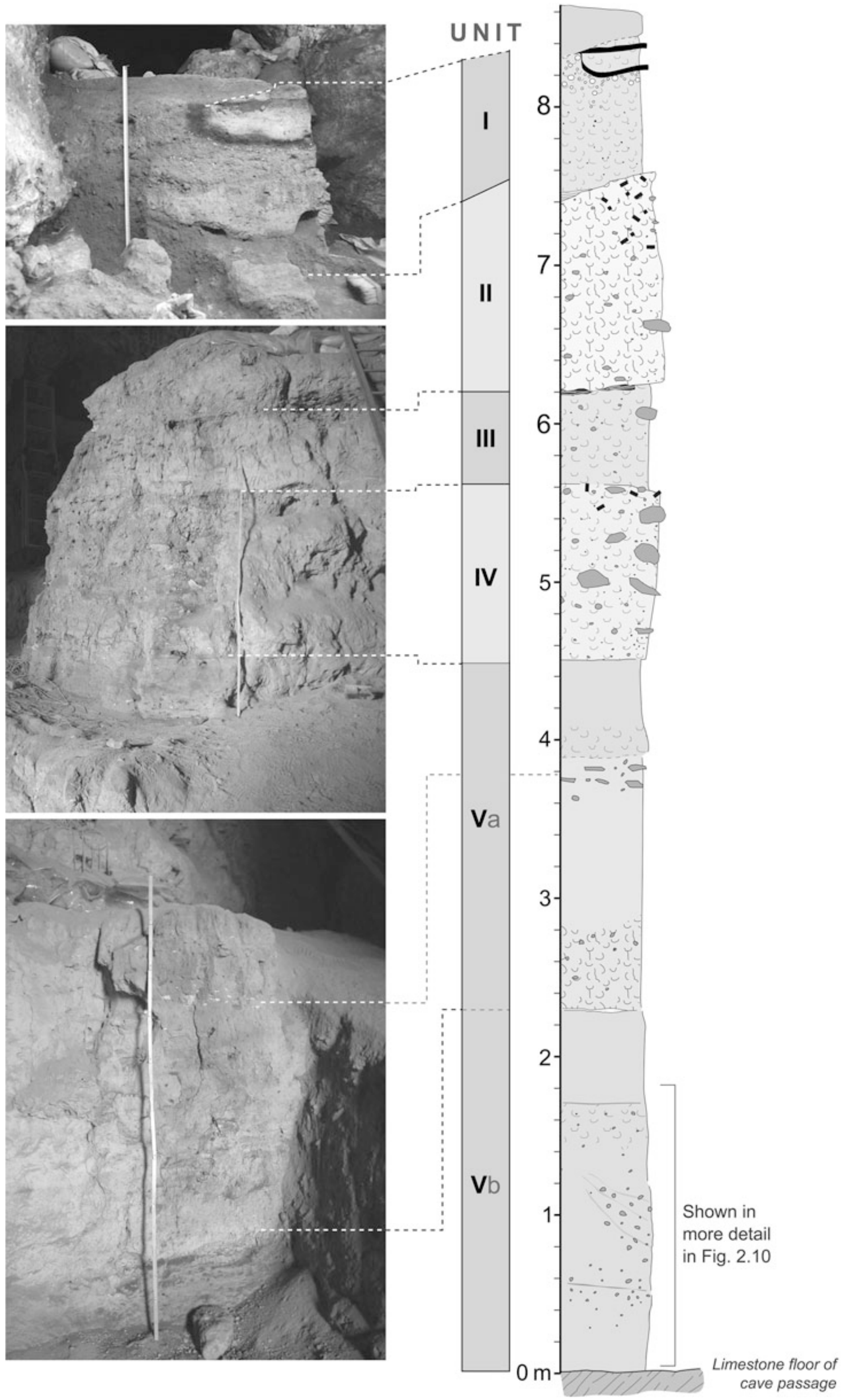

Fig. 2.6 Composite stratigraphic column for Sediment Sequence 2 in Azokh 1 passage. The height of the wooden ruler in the lower and middle photograph is 2 m whilst in the upper photograph the length of the tape is 88 cm. See Fig. 2.5 for a general sedimentological key. Modified from Murray et al. (2010)

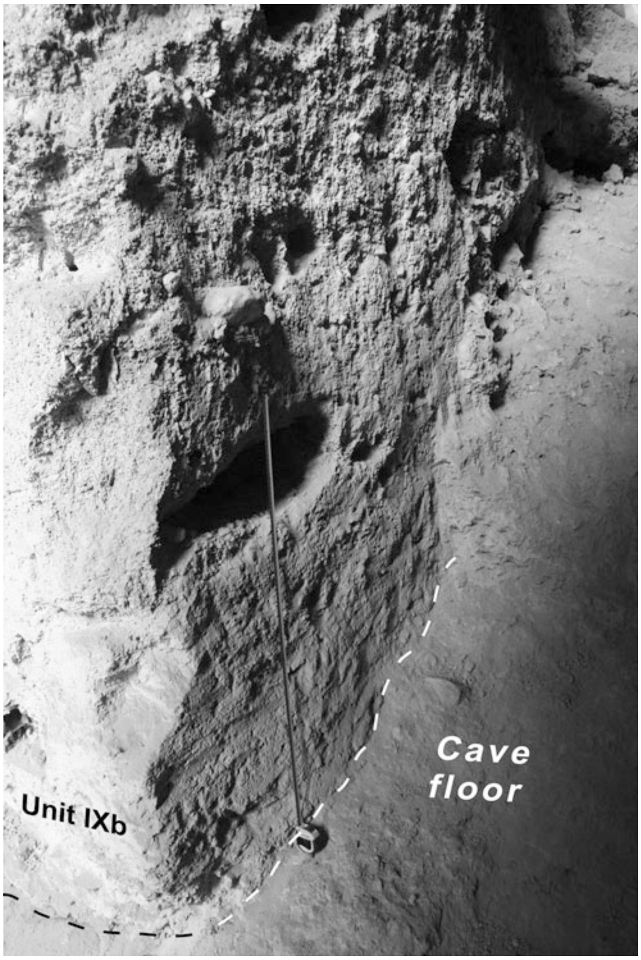

Fig. 2.7 Thinning of the base of what remains of Sediment Sequence 1 (Unit IX) which rests on the sloping cave floor. The tape measure (for scale) is showing 1 m

Fig. 2.8 Detail of the transition seen in the middle of Unit IX. The base of the unit (IXb) is more massive in character whilst the upper half (IXa) becomes progressively more granular in appearance towards the top of the photograph. The visible length of the scalebar is 86 cm

limestone boulder, which has presumably fallen into position from the cave roof. Excavation by previous teams around this collapse feature has resulted in the characteristic “mushroom” shaped pedestal close to the entrance to the passage (Figs. 2.4 and 2.5).

Fossils and lithic artifacts have not been observed or recorded so far in Units VII, VIII and IX. Given the limited extent of the remaining stratigraphy this is perhaps unsurprising and it partly explains why this portion of the succession remains largely undated (Table 2.1). Huseinov (1985) reported the recovery of very fragmentary fossils from this lower part of the stratigraphy, along with pollen. Clearly identifiable fossil fragments and charcoal are present in Unit VI towards the very top of Sediment Sequence 1. Murray et al. (2010) speculated that this divide between (largely) unfossiliferous and fossiliferous strata might be a reflection of a shift between the cave being closed during accumulation of most of Sediment Sequence 1 to a more open system towards the top. In particular, conglomeratic subunit VIc (Fig. 2.9) is unequivocally the product of energetic water flow through the passage (probably a small river) and the coincidence of this horizon with the first appearance of fossils supports this contention.

According to M.M. Huseinov (reported in Lioubine 2002), Sediment Sequence 1 equates to *“cultural”* layers V–VI (at the top) and VII down to X (below) [compare Fig. 2.5 herein to Fig. 8 of Lioubine (2002)]. Huseinov (1985) recorded over 200 lithic artifacts from layers VII–X (as he had interpreted the strata); however, the validity and stratigraphic integrity of these finds has subsequently been questioned and claims that they are “Lower Paleolithic” in character have been largely dismissed (Doronichev 2008; Doronichev and Golovanova 2010).

Fig. 2.9 Clast-supported subunit VIc conglomerate. Clasts are sub- to well-rounded. Scale bar is 21.5 cm in length

Sediment Sequence 2

This is a composite sequence that has been reconstructed from a series of vertical sections or "steps" (largely a by-product of the pre-2002 excavations) in the cave filling strata (Fig. 2.4). Sediment Sequence 2 can be subdivided into five constituent units (I–V; Fig. 2.6) totaling about 8.5 m in thickness. Over half of this thickness is accounted for by Unit V (approximately 4.5 m), which is located at the base. All five units of Sediment Sequence 2 have proven to be fossiliferous and much of the excavation work by the current team has been focused in this part of the succession.

Unit V is predominantly fine-grained in character and is divisible into two subunits: Vb (located at the base and largely non-calcareous) and Va (located directly above and calcareous in nature; see Table 2.1). It is likely that Unit V can be further subdivided beyond this two-part scheme; however, subunit Va presents a steep vertical face (just over 2 m; Fig. 2.6) in the section and, for safety reasons, it has not been possible to thoroughly examine the stratigraphy in detail.

Subunit Vb is best exposed in a small trench that was initially excavated through the Middle Platform in 2002 (Fig. 2.10; see also Fig. 2.4a for general location in Azokh 1 passage). Murray et al. (2010) described five horizons within this trench section and a refinement of some of their sedimentological details is outlined in Table 2.2.

The uppermost horizon (e) of subunit Vb can be traced laterally across the excavation surface of the Middle Platform and is seen to continue stratigraphically upwards for a further 35–40 cm. It is capped in places by a distinctive 1 cm-thick cream-white to white, non-calcareous phosphatic crust (see lowest photo correlation line at top of subunit Vb in Fig. 2.6), which forms a useful marker horizon.

Subunit Va is 220–230 cm thick and is predominantly composed of friable calcareous silty clay. The basal 55 cm is granular with common angular limestone clasts (2–10 mm), which are typically flattened parallel with bedding. The overlying 105 cm is more massive in structure and contains a distinctive horizon of flattened (cm-scale) clasts in the top third (see photo correlation line in Fig. 2.6). Charcoal was noted in this zone also. The uppermost 70–80 cm of subunit Va comprises friable calcareous silty clay. Its base is finely granular, however, its top is predominantly massive, lacks limestone clasts, and has a more reddish hue (resulting in 7.5YR rather than 10YR color designation; see Table 2.1). This subtle color transition is generally gradual in nature.

The contact between the top of Unit V and overlying Unit IV is diffuse; and is irregular and undulose when tracked laterally from the centre of the passage towards the cave walls. Where it is more clearly displayed it presents a subtle shift in

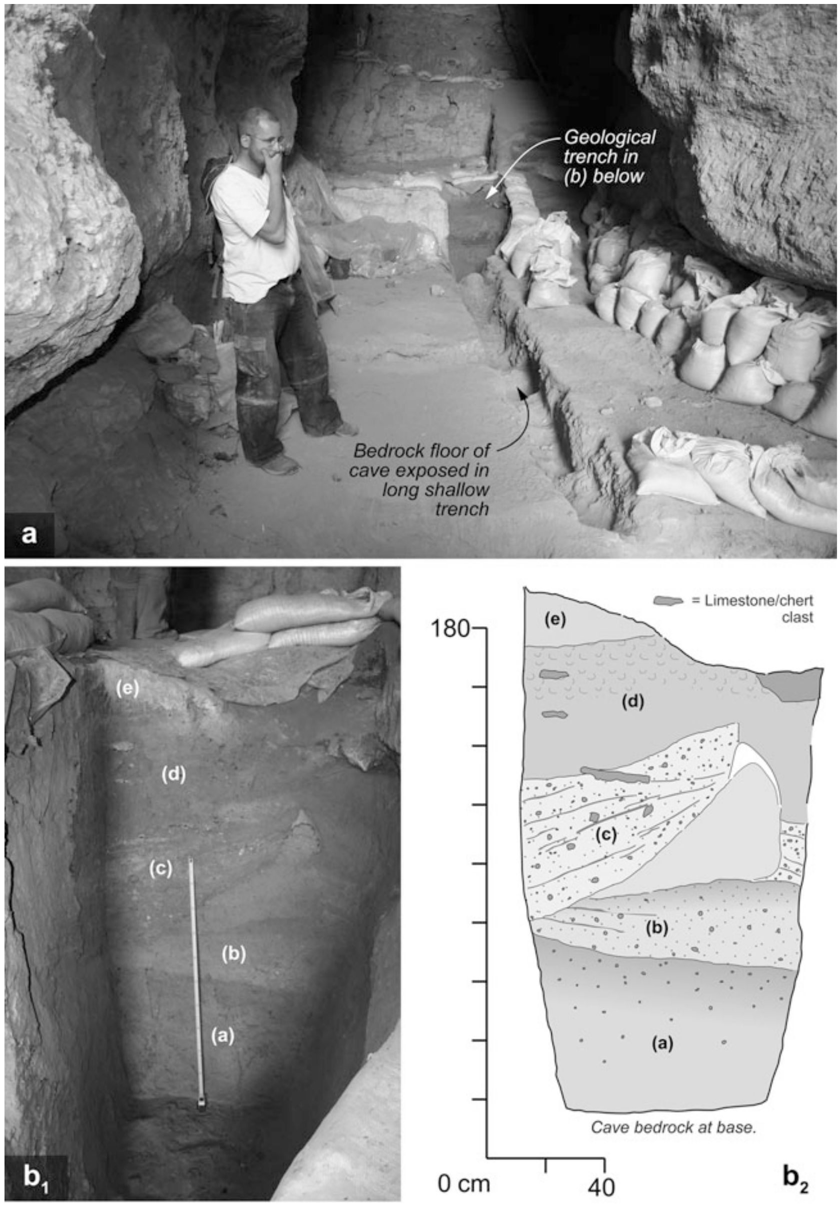

Fig. 2.10 The base of Sediment Sequence 2. **a** General location of the geological trench in the base of Unit V within Azokh 1 passage. This photo faces ENE and was taken in 2008, when the bedrock floor to the cave was found only a short distance below the (present) sediment level on the *"Lower Platform"*; $\mathbf{b_1}$ Photo and $\mathbf{b_2}$ corresponding scaled panel diagram of the sedimentary succession in the geological trench. A description of horizons (a) to (e) is provided in Table 2.2. Tape measure in $\mathbf{b_1}$ is showing 1 m. $\mathbf{b_2}$ is modified from Murray et al. (2010)

texture (moving upward from predominantly massive to fine granular) and color (the "reddish" 7.5YR top of Va is overlain by 10YR Unit IV; see Table 2.1). A characteristic feature of Unit IV is a progressive increase in flattened sub-angular to rounded (cave-wall) pebbles and cobbles towards the top of the unit, along with fragments of bone and charcoal.

When examined in the centre of the passage, the contact between Unit IV and (overlying) Unit III is quite obvious and sharp (see relevant photo correlation line in Fig. 2.6) and is marked by a shift in structure and a noticeable decrease (in Unit III) in the limestone clast content of the sediments. However, the contact has proven difficult to trace laterally when moving away from the centrally positioned reference section. At the time of writing, detailed excavation has begun to reveal more (from a lateral perspective) of this transition and it is likely that a reassessment of this particular contact may have to be made with new exposure. A possible two-part subdivision of Unit III into a lower (largely) massive subunit and an upper weak to moderate granular subunit is also becoming apparent.

Table 2.2 Subunit Vb succession evident in geological trench, Middle Platform, Azokh 1

Subunit	Horizon	Thickness	Consistence & Texture	Color	Rocks/clasts/comments	Carbonates
Vb	(e)	c. 20 cm (*In trench*)	Very firm clay loam	7YR 4/4 (Brown)	Contains common small soft (decalcified) white carbonate granules	Very weakly calcareous
	(d)	40–47 cm	Friable-loose clay loam	7YR 4.5/4 (Brown)	Angular limestone clasts are common, but dispersed. The base is massive, becoming weak granular towards the top	Non-calcareous
	(c)	50–0 cm (*Tapers out*)	Firm loamy sand	10YR 5/3.5 (Brown)	Forms a conspicuous "channel" structure in the section. Granule and pebble-scale clasts common, including angular dark chert clasts in matrix	Non-calcareous
	(b)	c. 20–30 cm	Friable loamy sand at base passing upwards into clay loam	Top:10YR 5/3 (Brown) Base:10YR 6/3 (Pale brown)	Noticeable gravel content. Internal stratification evident with a color gradation from the base to top (where it is darker)	Non-calcareous
	(a)	50–56 cm	Friable-firm sandy loam to loamy sand	10YR 6/3 (Pale brown)	Horizon rests directly upon the floor of the cave	Non-calcareous

Fig. 2.11 Lateral view of contact between Units III and II, Azokh 1. Hammer (arrowed) for scale

The contact between Unit III and (overlying) Unit II is conspicuous and is defined by a marked increase in the granularity of the sediments (Fig. 2.11). Murray et al. (2010) noted reddish-brown staining along this contact close to the northwestern wall of the chamber. Analysis of red- and orange-stained sediment from several units in Azokh 1 using Raman spectroscopy indicates the presence of fine-grained hematite and magnetite within the sediment (see below for further discussion). Subsequent excavation of the Unit III/II boundary has shown the hematitic staining to be more laterally widespread and the irregular nature of the contact to be more pronounced than initially thought.

Unit II rapidly (and somewhat irregularly) becomes non-calcareous upwards and also contains an elevated amount of limestone clasts (0.5–5 cm). These clasts, along with fossil bone fragments, are often strongly degraded, particularly in the non-calcareous zones. The deterioration of bone material within Unit II has been linked to accumulations of bat guano during its deposition, resulting in a non-calcareous, more acidic sediment (Murray et al. 2010). These authors reported the detection of tinsleyite (K and Al-rich hydrated phosphate) in the sediment. This particular mineral phase likely reflects syn-diagenetic processes where phosphatic mineralisation can precipitate due to the presence of bat guano (Magela da Costa and Rúbia Ribeiro 2001; Marincea et al. 2002; Shahack-Gross et al. 2004). It is evident that there is considerable lateral heterogeneity within Unit II in terms of its consistency, texture, geochemistry and the quality of taphonomic preservation (personal observations; see also Smith et al. 2016 and Marin-Monfort et al.

2016). Unit II was initially examined in a small cut section, near the Upper Platform and adjacent to the northern wall of the cave passage, where it measured c. 120–140 cm in thickness. More recent investigations of newly exposed surfaces of the Unit III/II contact in a more central position within the chamber, and also the overlying Unit II/I contact located approximately five meters deeper within the cave passage, have suggested potential thickness variation for Unit II of 150–200 cm. However, since these contacts are exposed in different positions within the passage, and neither section reveals Unit II in its entirety, it is unclear whether the thickness disparities inferred (from the differences in the elevations of the contacts) reflect real lateral thickness variation, or simply a slope in either/both of the unit boundaries towards the cave entrance.

The contact between Units II and I is sharp and irregular when traced out in detail, and the latter appears to infill the uneven topographic surface of the former. Unit I, which caps the entire cave-fill succession, is non-calcareous and predominantly a friable to loose clay loam. Excavation work on the Uppermost Platform (Fig. 2.4a) has shown this unit thins from more than 135 cm to between 80 and 90 cm towards the interior of the cave. A reference section for Unit I has been preserved in the rear of Azokh 1 passage (Fig. 2.12). Murray et al. (2010) noted that this particular section demonstrated two key features:

- Considerable disturbance and reworking of the sediment by recent mammal burrowing activity. Fossils of *Ursus spelaeus* and coprolites, as well as Paleolithic stone tools have been recovered from these burrows (Marin-Monfort et al. 2016). This large-scale bioturbation has served to greatly complicate the internal stratigraphic details of Unit I.
- Close to the top of the unit a conspicuous c. 30–40 cm thick fumier (manure hearth) occurs (Fig. 2.12; see also Fig. 2.6). This feature consists of a series of black, carbon-rich bands with greyish-white ash-rich interlayers. Dispersed, but common, soft white carbonate granules (occasionally these are decalcified) in the top 35 cm of Unit I may possibly be related to the heating effect of this large hearth structure on the surrounding sediment.

A conspicuous component of several of the stratigraphic units within Azokh 1 is the presence of disseminated clay-like pedofeatures within the sediment groundmass (Fig. 2.13). These features typically occur as millimeter- to centimeter-scale, sub-circular to lensoidal nodules and disseminated specks, as well as thin (c. 1–3 mm) discontinuous sub-horizontal seams (typically 1–5 cm long). They are composed of fine-grained (<0.05 mm), white to buff, powdery, clay-like material and generally do not display any internal banding or lamination. Similar clay-like material also forms partially developed concentric laminae within and around decomposing bone fragments in the sediment (Fig. 2.13d). The occurrence of these nodules appears to begin within Unit VI at the top of Sedimentary Sequence 1 and remains variably developed, moving up the stratigraphy, throughout Sedimentary Sequence 2 (Units V–I). This distribution appears to broadly correlate with marked increases in numbers of fossils and the calcareousness of the sediment (see Table 2.1).

The analysis of nodule material was performed using Raman spectroscopy in an attempt to characterize its mineralogy/composition and help identify a likely formational mechanism. Representative material was sampled from several stratigraphic horizons (e.g., Units VIa, VIb, Va, Vb and IV; Fig. 2.13) and analyzed following the procedure outlined in the Spectroscopy Methodology section (preceding the references). Preliminary results indicate that the nodules are predominantly composed of fine-grained phosphatic material including apatite and/or hydroxylapatite (Fig. 2.14). Representative Raman spectra display strong peaks shifts in the range 967–1020 cm^{-1}, diagnostic of phosphatic minerals (e.g., Sinyayev et al. 2005; Kizewski et al. 2011). The variation in the width of these Raman peaks for phosphates likely reflects a spectroscopic response between crystalline phases (narrow peak) and more amorphous mineral forms giving broader peaks (cf. Fig. 2.14).

The likely provenance of the phosphatic nodules includes the weathering of bone material, as evident by its association with partially decomposed bone fragments (Fig. 2.13a, d), and/or diagenetic formation following the syn-sedimentary accumulation of bat guano and a subsequent increase in the concentration of dissolved phosphate within infiltrating aqueous fluids (e.g., Karkanas et al. 2000, 2002; Shahack-Gross et al. 2004). Thus, the nodules appear to be autochthonous and formed as a result of post-sedimentation weathering/alteration and diagenetic processes resulting in the formation of authigenic phosphate. This hypothesis is supported by the general disseminated, undeformed and granular appearance of the nodules that display little evidence of mobilization or re-working.

Additional diagenetic features of the sedimentary sequence within Azokh 1 include the occurrence of rust-red to orange-brown colored staining, coatings, nodules and grains throughout the succession (Fig. 2.13e, f). Raman analysis of representative orange-stained sediment and sub-rounded nodules and specks from Units IXa, IXb and Vb indicates that this material is primarily of iron oxide composition and is dominantly hematite with lesser magnetite (Fig. 2.14).

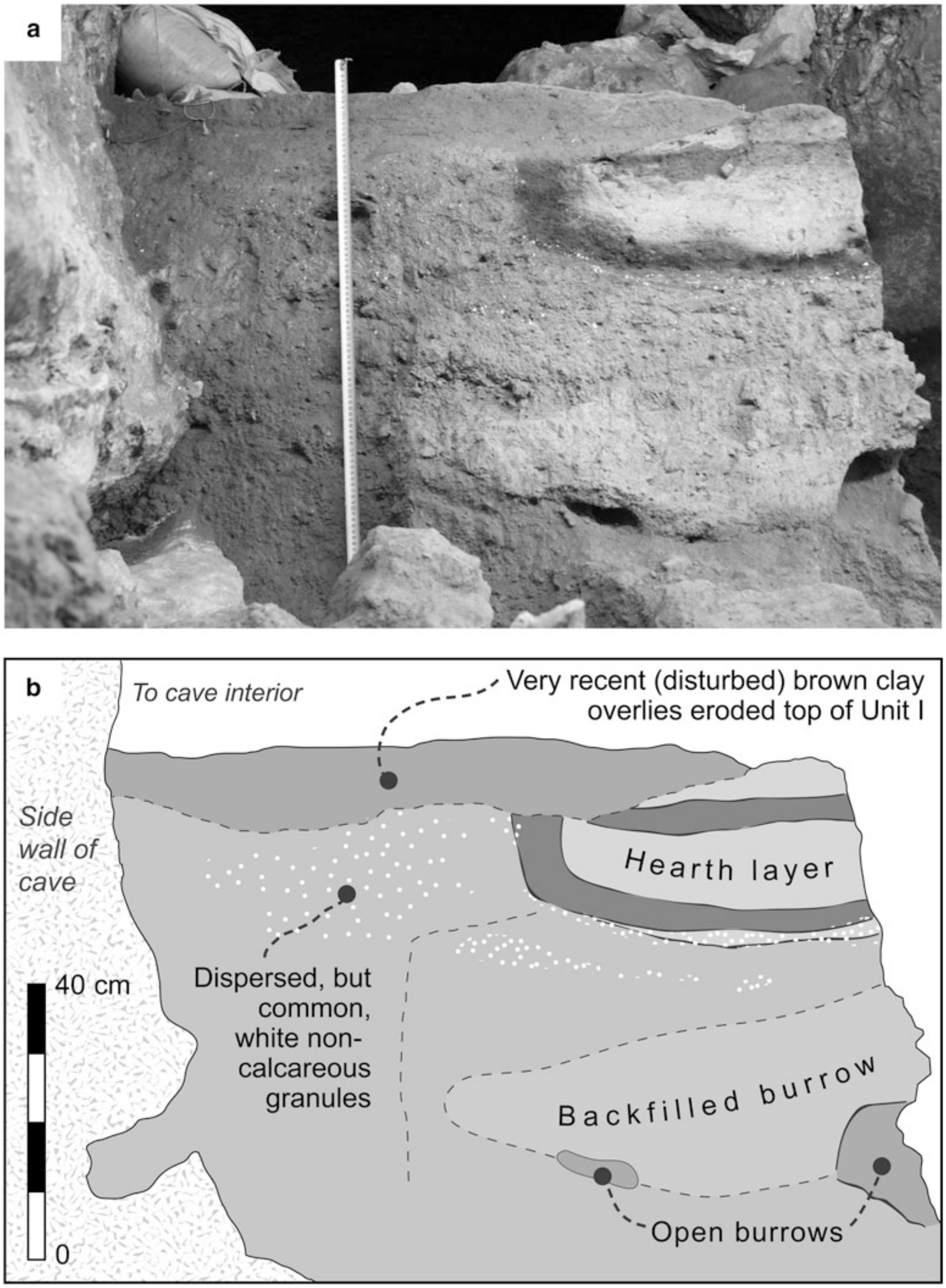

Fig. 2.12 **a** Photograph of the top of Unit I after it was exposed and cleaned during the 2007 field season. The visible length of the tape measure is 88 cm. **b** Sketch interpretation of the photograph in (**a**) showing hearth layer (fumier), disturbance by burrows and eroded top of Unit I. Reproduced from Murray et al. (2010)

Dating and Correlating the Sediment Sequences

A range of radiometric dates for Sediment Sequence 2 is reported in the Appendix of this volume. Age determinations are included here and also summarized in Table 2.1. Moving from the base to the top of the sequence:

Units V and IV: Uranium series dating suggested an age of c. 200 ka for Unit V, whilst racemization (D/LAsp) indicated an age closer to 300 ka. However, the most up to date ESR estimate indicates an age of 293 ± 23 ka. An ESR date of 205 ± 16 ka has been calculated for the base of Unit IV, very close to the contact with underlying Unit V.

Unit III: No dates are available for this unit.

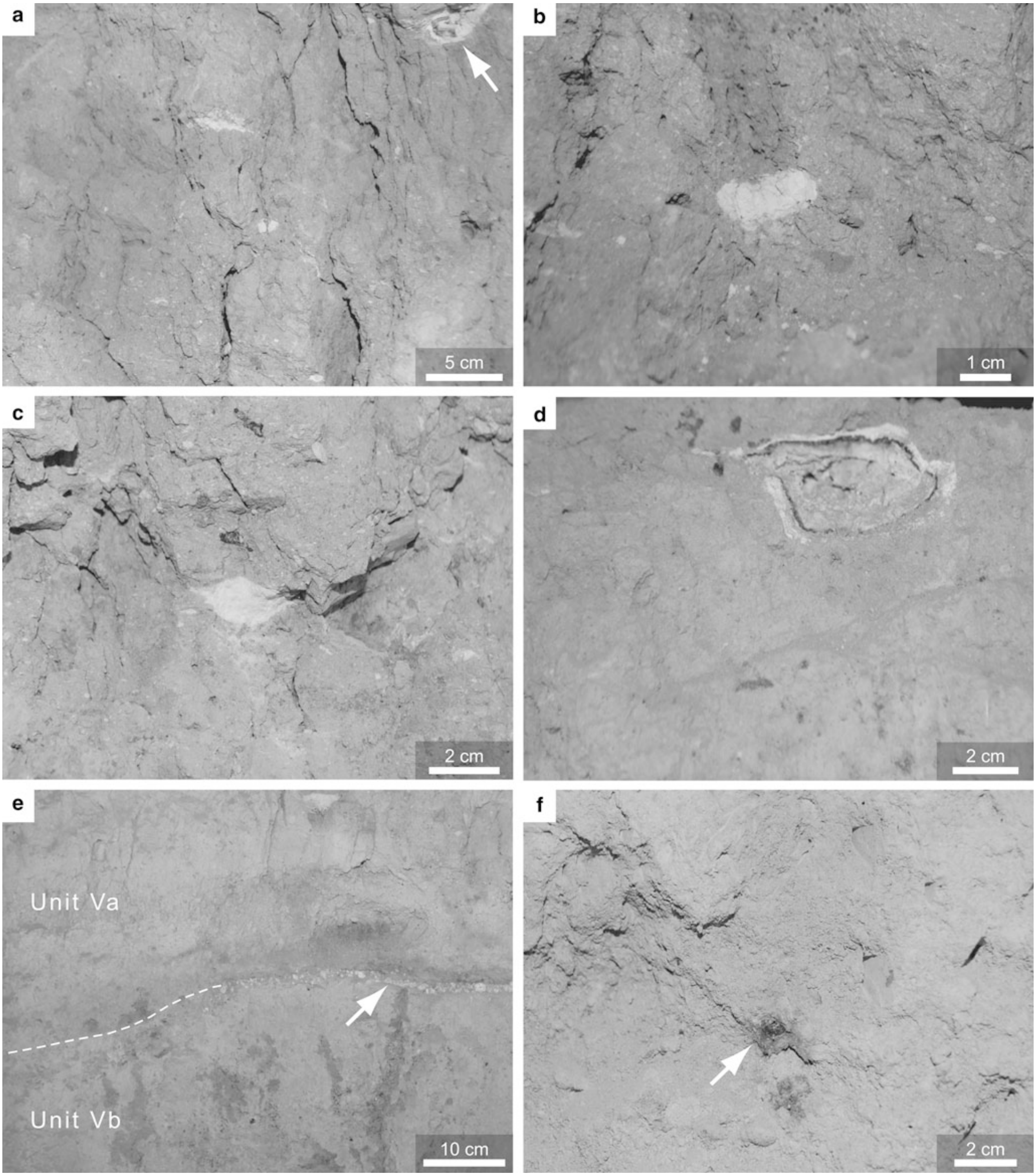

Fig. 2.13 **a** Phosphate nodules in Unit VIa. Nodules occur as cream to white, clay-like lenticular concretions and disseminated specks, or as partially developed concentric laminae within decomposing bone material (arrowed). **b**, **c** Detailed views of phosphate nodules disseminated in Unit VIa. In (**c**) the lenticular form of the nodule in the center of the image is similar to the shape of the bone material shown in (**a**) and (**d**). **d** Partially decomposed bone fragment in Unit Vb displaying concentric phosphate (white) and hematite (dark grey) banding. **e** Contact between Unit Vb and Va partially defined by a 1 cm nodular seam of phosphatic material (arrowed). The dark grey, sub-vertical patches seen in Unit Vb represent hematitic-stained sediment. View looking approximately east. **f** Rounded hematite nodule in Unit IXa (arrowed)

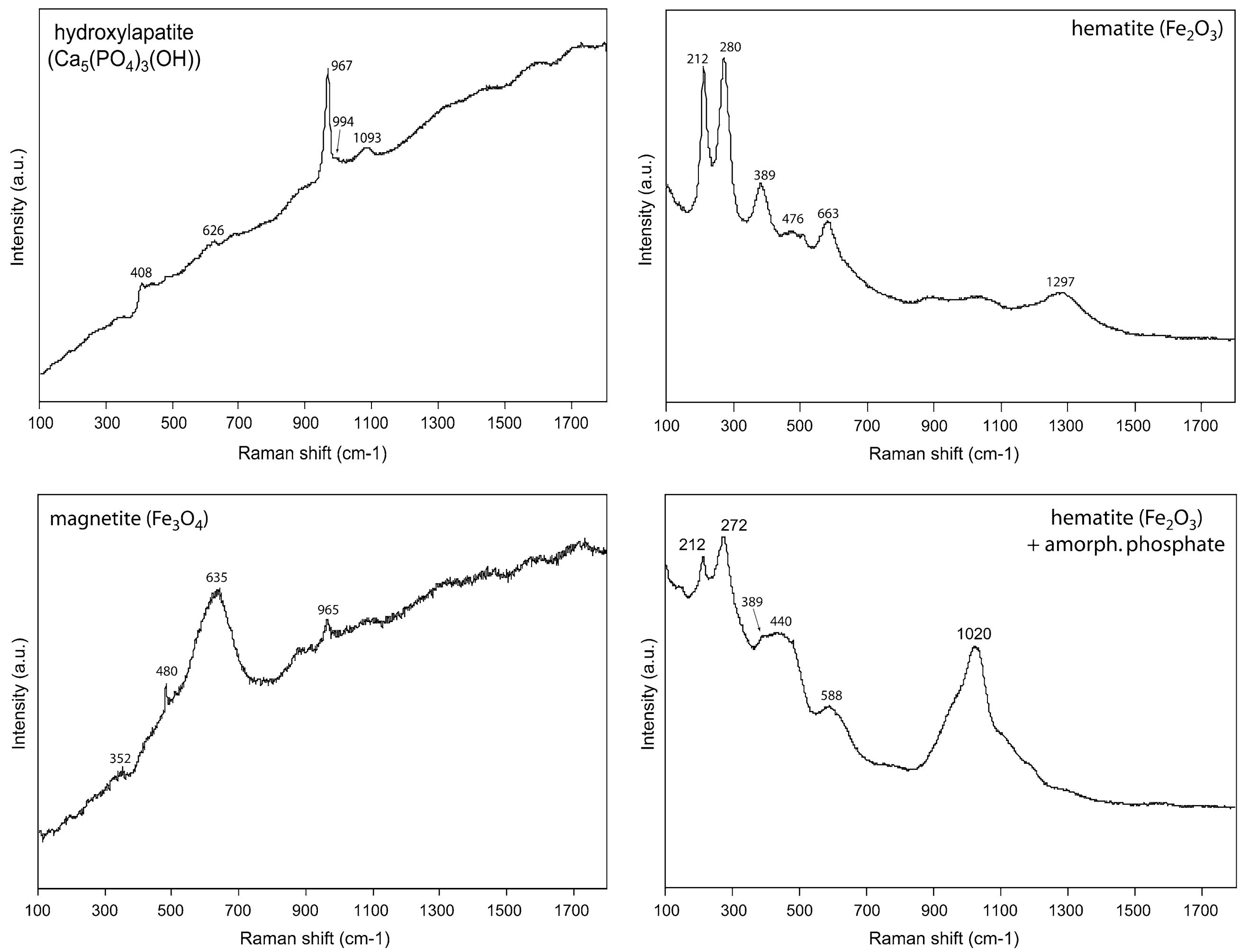

Fig. 2.14 Representative Raman spectra of mineral phases present within several Azokh 1 sedimentary units. Diagnostic peak positions are labeled using Raman shift values (cm^{-1}). Raman intensity is in arbitrary units (a.u.)

Unit II: Murray et al. (2010) noted an unsuccessful attempt to radiocarbon date this unit and suggested its age likely exceeded the lower radiocarbon range of 60 ka. Subsequent ESR dating has provided an age of 184 ± 13 ka for the base and 100 ± 7 ka for the top of Unit II (see Appendix, ESR).

Charcoal from the fumier in Unit I provided a radiocarbon age of 157 ± 26 ^{14}C BP (see Appendix, radiocarbon). Murray et al. (2010) noted that a Russian coin, from around the mid-1960s, was discovered in 2006 (although it had been moved by subsequent bioturbation). Below the hearth in Unit I, the sediments are highly disturbed (Fig. 2.12), so confident dating this unit remains problematic.

It is clear that Sediment Sequence 2 ranges in age from Middle to Late Pleistocene (Units V to II; Table 2.1). The Middle Pleistocene age for Unit V is significant as it is from this level in the succession that the hominin mandible was recovered in the 1960s (Kasimova 2001; see also King et al. 2016). The sharp, irregular contact between Units II and I at the top of Sequence 2 is disconformable and may represent a hiatus in sedimentation, with possible subsequent erosion, between Late Pleistocene and Holocene times (Table 2.1). This relationship suggests that the Pleistocene-Holocene boundary transition is not fully represented in the succession (Murray et al. 2010).

The details of the age of Sediment Sequence 1 remain unclear. Attempts to resolve the matter are hampered by two principal factors:

1. *The limited extent of the remaining stratigraphy*. This has already been discussed, but the lack of fossil remains and bona-fide lithic artifacts in Units IX to VII is also problematic.

2. *Uncertainty in how the two sediment sequences precisely correlate.* This is a function of the fact that no *in-situ* sediment connection now remains between the two sediment sequences in Azokh 1. The simplest view of the situation (Occam's razor) would be to assume that Sediment Sequence 1 is positioned at a lower level in the passage (Fig. 2.4) and therefore must stratigraphically (directly) underlie Sediment Sequence 2. However, with the lack of information about the lateral connection of strata, it is impossible to establish with any degree of certainty if the cave-fill sequence is progradational. The presence of conglomeratic subunit VIc (Fig. 2.9) signifies a period of increased water flow through the passage. This may have eroded parts of any pre-existing strata, introducing a time gap of unknown duration into the sequence, casting an element of doubt into the assumption that Sediment Sequence 1 records a smooth, unbroken succession from Middle Pleistocene (near the top) to older times (moving stratigraphically downwards).

Correlation between the two sediment sequences in Azokh 1 is discussed in detail by Murray et al. (2010), who propose several possibilities:

- Using the bedrock floor of the cave as a datum, the base of subunit Vb in Sequence 2 is equivalent to the base of subunit VIc or possibly even the upper portion of Unit VII in Sequence 1.
- The highly conspicuous conglomeratic subunit VIc in Sediment Sequence 1 (Fig. 2.9) may correlate with the lenticular unit (horizon (c) in Fig. 2.10b) in the base of Vb. The latter displays an erosive, channel style geometry and exhibits an elevated gravel content. Although the sedimentological details of the two units are not identical, both *could* have been produced by fluvial processes and the differences between the two may be a reflection of lateral facies variation.
- The increase in calcareousness in the units overlying conglomeratic VIc and horizon (c) in subunit Vb may provide grounds for a chemostratigraphic correlation. In Sequence 1, subunit VIb is mildly calcareous, whilst VIa at the very top of the preserved section is strongly calcareous (Table 2.1). A similar transition is seen towards the very top of subunit Vb in Sequence 2.

According to Huseinov (1985) paleomagnetic work on the sediments infilling Azokh 1 indicated that the bulk of the middle and upper part of the stratigraphy lies within the Brunhes Polarity Chron (i.e. dating back to 0.781 Ma). Huseinov (1985) noted though, that *his* "Layer VIII" (*very broadly* equivalent to the middle of Sediment Sequence 1, as defined herein) was reversely magnetized, suggesting possible placement within the Matuyama Polarity Chron. Ljubin and Bosinski (1995) also noted this possible magnetic reversal in the lower part of the succession. If this is indeed correct, it would imply that the very basal part of the stratigraphy of Azokh 1 is Early Pleistocene in age.

Discussion on the Stratigraphy of Azokh 1

Depending on the method of lateral correlation employed between the two sediment sequences, a total of between 11.2 and 12 m of stratigraphic infill can be accounted for in Azokh 1 passage. Much of this sediment has been removed by previous excavations (Fig. 2.4) and the lack of rigorous recording of this material compromises the information potential of the stratigraphic remnant described here. A graphic illustration of this is the confusion over the precise level within Unit V of the find of the partial Middle Pleistocene human mandible (see discussion in Murray et al. 2010 and references therein).

Lioubine (2002) noted that the "stepped back" appearance of the excavation in the passage (Fig. 2.4) severely hinders any potential study of paleoclimatic proxies, which are generally best preserved in the sediments close to the cave entrance. A similar argument can be made for evidence for human occupation and activity, which is usually best preserved near entranceways in cave settings. Uncertainty over the lateral connection of strata through the cave passage has already been discussed here. Lioubine (2002, p. 23) noted, for example, that Unit V apparently thinned dramatically from 5 to 2 m. This was based on a review of previous reports on the stratigraphy and, admittedly, more precise details were not available to him.

The distinction between the largely unfossiliferous Sediment Sequence 1 and fossiliferous Sediment Sequence 2 above is not easy to explain. It may be a taphonomic artifact; a result of the limited amount of stratigraphy remaining in Sediment Sequence 1 or it may simply be a function of accessibility, with the lower level of the passage (see "basal trench at cave entrance" in Fig. 2.4) not as easy to enter at the time it was originally infilling with sediment. Murray et al. (2010) also highlighted this fossiliferous distinction between the two sequences and tentatively suggested that this may reflect the degree to which the cave passage was open to the outside world. Conglomeratic subunit VIc (Fig. 2.9) is located at the top of this apparently unfossiliferous sequence. It is a particularly distinctive horizon that contrasts with the largely fine-grained units below and directly above. Sedimentologically, it represents a marked increase in the strength of water flow through the passage at this point and it may *possibly* be related to improved accessibility of the passage (discussed previously herein; see also commentary in Murray et al. 2010).

Sediment Sequence 2 dates from the Middle Pleistocene to the present (Table 2.1; see also Appendix of this volume); although the disconformable relationship between the top of Unit II and base of Unit I means the actual Pleistocene-Holocene transition is not represented. A rich and diverse Pleistocene fauna has been recovered from Units II–V and preliminary findings are listed in Fernández-Jalvo et al. (2010). Cave bears dominate the macro-mammal fraction (Van der Made et al. 2016), whilst bats are a common constituent of the micro-mammal component of the fauna (Sevilla 2016).

The sedimentological differences between the various units infilling Azokh 1 may reflect individual episodes of deposition and sedimentation in response to karst development and paleoenvironmental change, as opposed to a gradual evolution of the entire sedimentary sequence. Much of the sediment in Sequence 2 is quite fine-grained (see Table 2.1) suggesting generally low levels of depositional energy. However, two levels within this portion of the cave-fill (Units IV and II) contain elevated amounts of relatively coarse, angular, limestone debris (Fig. 2.6). Murray et al. (2010 [p. 87] and references therein) suggested that this could represent frost action during cooler climatic intervals but cautioned that other geomorphological processes, such as seismic activity, dissolution and hydration shattering, may produce similar results. These authors also noted that the slope of the various chambers and passages comprising the Azokh Cave system (Fig. 2.2) suggested water and fine-sediment flow from the interior towards the exterior. However; it is entirely possible that the patterns of sedimentation varied throughout the cave's history, with alternation between the two flow directions occurring. As noted in the opening paragraphs of this section, due to the fact that lateral facies changes were undocumented during the original excavation phase and the fact that the sediment is now removed, this will have to remain a point of conjecture.

Azokh 2

The entrance to the passage we have named Azokh 2 (Fig. 2.3b) is located approximately 42 m NNW from the Azokh 1 entrance (Fig. 2.2). The present level of archaeological excavation has resulted in a chamber that is accessible for about 7.5 m (length) by 3.5 m wide (Fig. 2.15), while the unexcavated level of sediment within the chamber begins approximately 2 m below the roof of the passage. A large boulder collapse has choked the rear, or northeastern end, of the passage where it leads into the interior of the cave (Fig. 2.15; see also Fig. 2.2). This blockage has been a hindrance to further exploration and excavation work within this passage. Azokh 2 is sunlit during daylight hours.

Two geological test trenches (see Fig. 2.15) were dug in 2002 [Pit 1] and 2003 [Pit 2] to begin investigating the stratigraphy of the sedimentary infill of Azokh 2. This preliminary work sub-divided the sediments into two stratigraphic units which are readily distinguishable on the basis of color. The lower Unit 2 is light yellow-brown in color, which contrasts sharply with the dark greyish-brown appearance of Unit 1 above. Details of the findings of that work are summarized in Table 2.3. Measurement of the elevation of the contact between the two units (below the level of the cave datum) exposed in the two test pits suggested a possible slope of c. 10° towards the southwest (i.e. towards the cave exit; Fig. 2.15). This slope is less apparent when examined in detail near the entrance to the passage.

Unit 2 is at least 90 cm thick (the base was not seen) and can be divided into a lower subunit with rare limestone clasts (2b) and an upper subunit with an increased proportion of limestone clasts (2a). Unit 1 is considerably more complex and heterogeneous in character. A subtle shift in granular structure of the sediment effectively marks the distinction between its two constituent subunits (Table 2.3), although this is not always apparent when traced laterally. Unit 1 contains numerous hearth layers, particularly in subunit 1b. These are commonly white to light grey and ashy in appearance, with an associated reddening of the surrounding sediment.

In 2007 the two test excavation pits in Azokh 2 were reopened in order to excavate the intervening sediment section (see details on Fig. 2.16) and during this work, modern human postcranial skeletal remains were discovered. This particular find was reported by Fernández-Jalvo et al. (2010), who noted an age estimate of 1265 ± 23 ^{14}C BP.

Discussion on the Stratigraphy of Azokh 2

Knowledge of the stratigraphy of Azokh 2 is still very much at a preliminary stage. This is largely a function of the boulder choke at the rear of the passage (Fig. 2.15) that has imposed a physical restriction on the direction and degree of

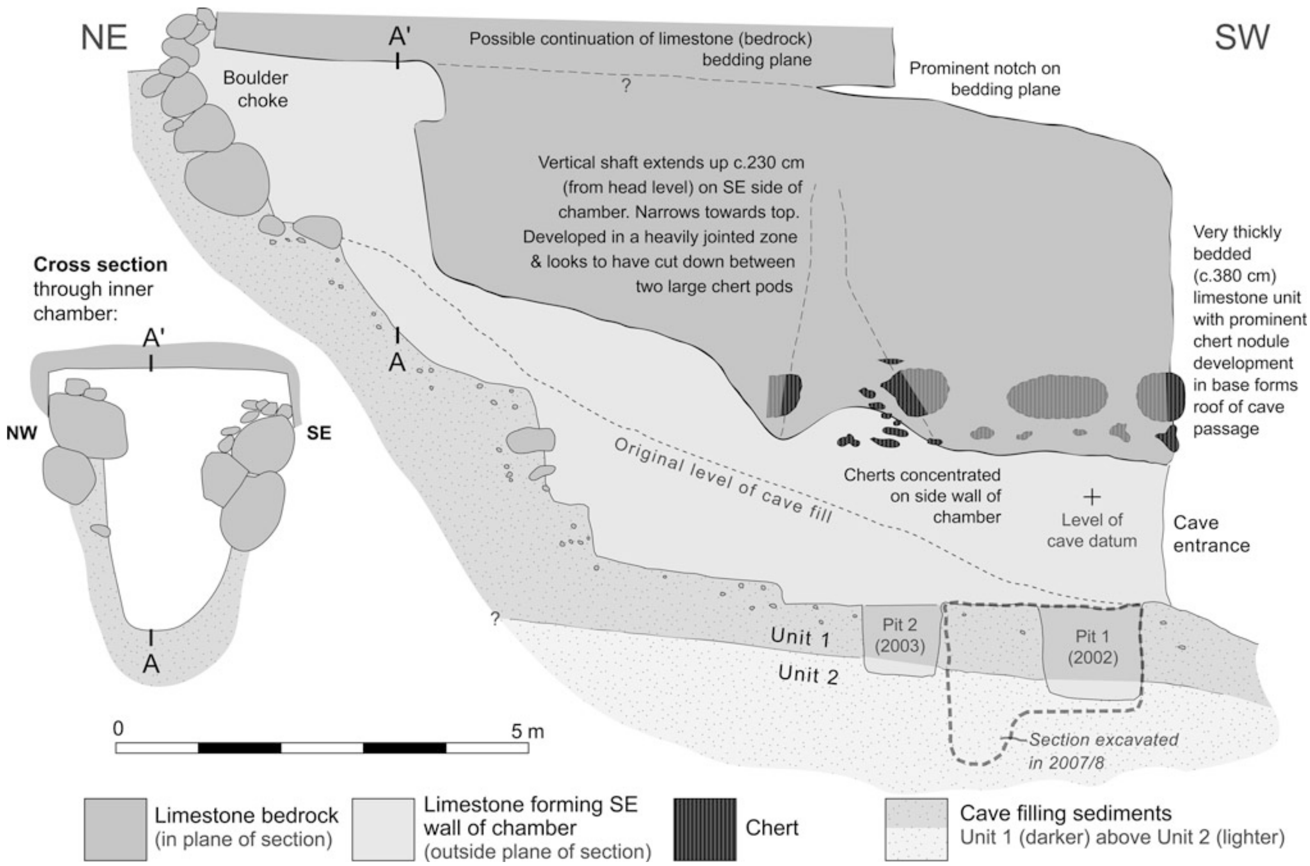

Fig. 2.15 Sketch cross-section through the Azokh 2 chamber (drawn facing SE). The locations of various trenches developed over several field-seasons (2002, 2003 and 2007) are indicated. Note that the SE walls of these trenches are out of the plane of section and are thus unornamented. Note also the original level of cave fill prior to the current phase of excavation and the boulder filled inner chamber in the rear of the cave passage

excavation work possible. The possible distinction between the two sedimentary units may possibly reflect the passage shifting from a closed (Unit 2) to a more open (Unit 1) system. The increase in the abundance of limestone clasts between subunits 2b and 2a (above) may represent a gradual shift towards wetter and/or cooler climatic conditions, but this remains debatable (see discussion on coarse limestone debris in sediments in Azokh 1 above).

The overlying sediments of Unit 1 are conspicuously more humic and organic rich. They are noticeably heterogeneous when tracked laterally and the presence of numerous hearth layers attest to a sustained period of past human activity in the passage. The first hearth layer appears directly on the contact between Units 1 and 2, which may possibly support the contention that humans only entered the passage when it became open to the outside world. The age of the underlying Unit 2 is uncertain since no artifacts or fossil remains have been recovered from this unit.

Azokh 5

The entrance to the Azokh 5 passage is located about 100 m NNW from Azokh 1 and it connects to one of the largest inner chambers of the Azokh Cave system (Chamber IV; see Fig. 2.2 and also Domínguez-Alonso et al. 2016). The roof of the entrance passageway bears morphological characteristics suggestive of formation as a phreatic tube (Fig. 2.3c). This passage continues northeastwards from the entrance for 5 m before rapidly opening upwards and outwards, creating an inner sub-chamber (Fig. 2.16) which has a significant sediment infill. Chert development is quite prominent in the limestone forming the roof to this connecting passage.

Excavation and investigation of the stratigraphy in Azokh 5 has been conducted intermittently since 2006. The *in situ* sediments were covered by a ramp of mixed sediments containing, amongst other things, human teeth and tools, as well as additional fauna (see Fig. 2.16 for an indication of the

Table 2.3 Stratigraphy of Azokh 2 Passage

Unit/ Sub-unit		Thickness	Consistence & Texture	Structure	Color (Munsell)	Rocks/clasts/comments	Carbonates
1	1a	20 cm (*Present in trench, but thickens considerably in direction of cave interior – the top of this unit was not seen*)	Friable-firm clay to silty clay	Fine granular to massive	10YR 4/2 (Dark greyish brown)	(In logged section): Matrix-supported greyish angular limestone clasts (up to 21 cm across) and abundant recent plant rootlets. Charcoal fragments noted near base. Boundary with underlying subunit is topographically irregular. Above this level, this subunit currently includes the thick (mixed and disturbed) deposits of the boulder collapse at the rear of the passage	Calcareous
	1b	c. 55–60 cm	Friable silty clay	Medium granular	10YR 3.5/2 (Dark greyish brown)	Angular grey limestone clasts dispersed throughout, but they are particularly concentrated in the basal 25 cm on the WNW wall of the trench (i.e. closest to the cave wall). Recent plant roots penetrate this layer. This horizon is quite heterogeneous laterally and vertically. A prominent 3 cm thick pale grey ash layer (hearth) was located 7 cm from the top of this subunit. It dipped gently in a southerly direction (i.e. the direction of the cave entrance) and passed laterally into a unit with abundant flecks of charcoal. Charcoal was concentrated (broadly) in the top 20 cm of the subunit as a whole. Pottery fragments were recorded in this upper zone also	Calcareous
2	2a	c. 40 cm	Friable sandy/silty clay	Largely massive, granular in places	10YR 6/4–6.5/4 (Light yellowish brown)	Sub-rounded to angular limestone clasts common. Limestone clast content increases gradationally across contact with subunit 2b below	Strongly calcareous
	2b	50 cm+ (*Base not seen*)	Firm clay (*With minor sand/granule component*)	Massive	10YR 6/4 (Light yellowish brown)	Limestone clasts generally rare	Strongly calcareous

original level of cave fill). A 145 cm deep trench [Pit 3] in the entranceway to the chamber (Fig. 2.17; see also Fig. 2.16 for general location) revealed the following stratigraphy:

1. [Top]: 45 cm (minimum) very weakly calcareous medium-brown clay-rich soil (humus). A very strong granular structure was developed and many modern plant rootlets were present throughout. Angular limestone clasts (on all scales) were dispersed throughout, and gastropod shells and bat bones were also present.
2. [Middle]: 62–70 cm light beige-yellow firm calcareous clay, with a noticeable carbonate sand and granule component. Scattered limestone and (angular) chert clasts (generally 2–7 cm) were present; however, they were less abundant in comparison to unit 1 above. A moderate to strong granular texture was developed.
3. [Base]: 30 cm (minimum – base not seen) medium reddish-brown calcareous silty clay. It was reasonably well sorted with a moderate to fine granular texture.

Currently, five sedimentary units (labeled A–E) have been identified in the inner chamber (see Table 2.4 and also Figs. 2.16 and 2.18), comprising a predominantly fine-grained succession that is punctuated by two horizons containing elevated amounts of coarser clasts (Units B and D, see Table 2.4, Fig. 2.18). The larger clasts in these layers comprise limestone and chert debris, some of which appears to have simply dropped from the roof above. The significance of these two horizons with elevated amounts of coarse angular cave-wall debris may be that they indicate a shift towards wetter or cooler conditions, but (as discussed above for both Azokh 1 and 2) this line of reasoning is somewhat speculative. The stratigraphic horizons which directly follow Units B and D (Units A and C respectively) both drape and infill their irregular top surfaces.

The contact between Units A and B (at the top of the inner chamber sequence in Azokh 5) is both conspicuous and significant. The top surface of Unit B is quite irregular and rough and is progressively infilled by the laminated fine clays and silts of Unit A. Thin seams of fine to medium sand-grade material also occasionally occur in the latter. Unit A represents a switch to calcareous sediment deposition within Azokh 5 (Table 2.4).

The sedimentary laminations of Unit A are inclined and appear to have banked up in this corner of the chamber,

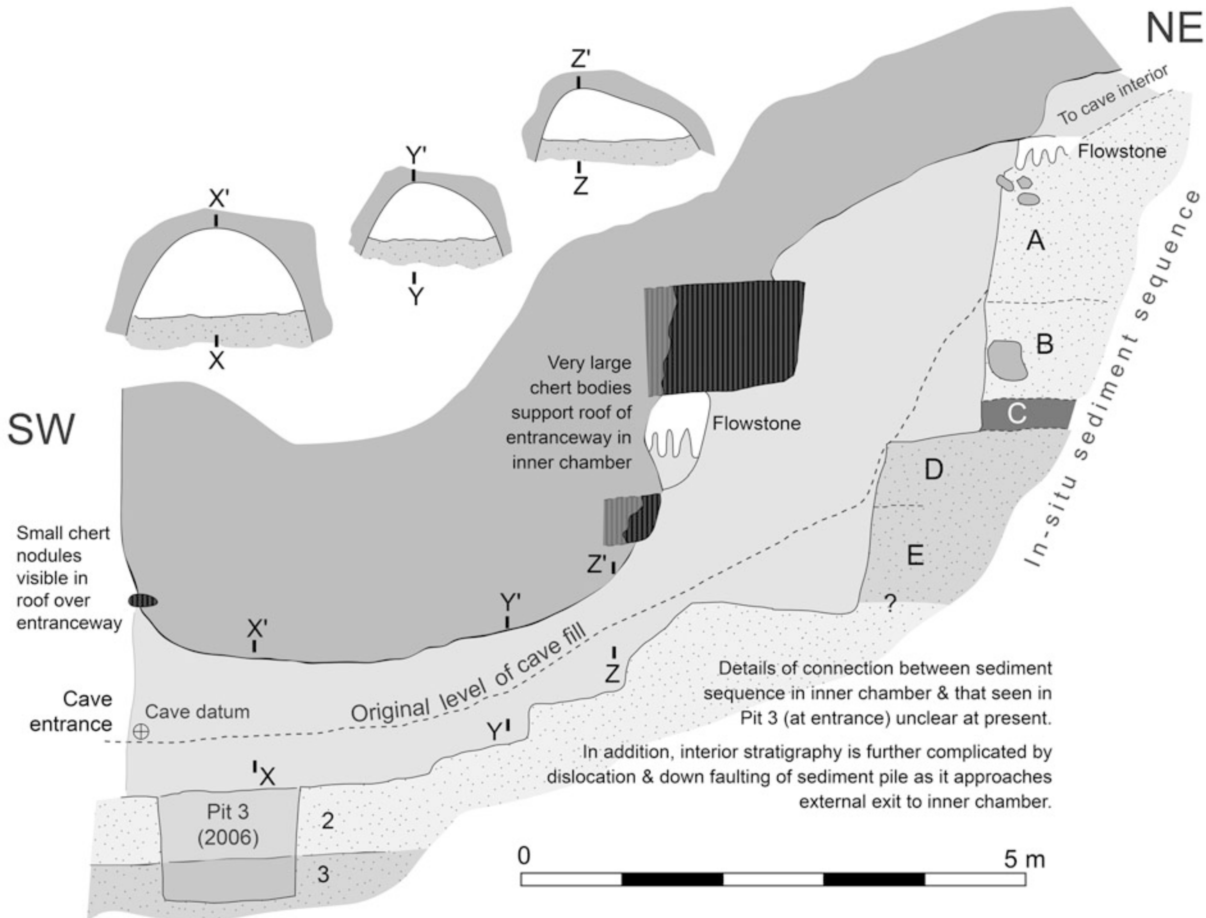

Fig. 2.16 Sketch cross-section through the Azokh 5 chamber (drawn facing NW). The locations of Pit 3 and the *in-situ* sediments exposed in the inner chamber are indicated. The NW wall of Pit 3 is out of the plane of section and is thus unornamented. Note the original level of cave fill prior to the current phase of excavation. Three consecutive cross-sections (*X*, *Y* and *Z*) illustrating the profile and shape of the entrance tunnel are presented. These are drawn to the same scale as the main section. These sections were drawn before any systematic excavation took place in Azokh 5, and consequently the level of sediment fill corresponds with the dashed "original level of cave fill" line. For key to ornaments see Fig. 2.15

effectively onlapping the top of Unit B. This may have introduced a time gap of unknown duration into the sequence. Fernández-Jalvo et al. (2010) reported modern human remains (teeth and cranial fragments) with associated charcoal from Unit A. The latter provided a radiocarbon age of c. 2.3 ^{14}C kBP. These authors suggest a possible relationship between this material and finds from near the base of Unit I in Azokh 1. It is interesting therefore that both Unit A (Azokh 5) and Unit I (Azokh 1) have discordant relationships with the units they succeed and both infill irregular topographic surfaces of their respective underlying strata. However, despite these general similarities, and in the absence of criteria allowing direct and precise correlation, any broad correlation in terms of the infilling history of the two passageways remains entirely hypothetical.

Unit B thins to 34 cm in the northwestern corner of the chamber and is covered and cemented on the upper surface by flowstone. A mineralised cylindrical structure, possibly a calcified mammal burrow (Fig. 2.19), occurs just below this level. Flowstone has also been observed in association with Units A and D, suggesting that this portion of the cave has remained wet for some time.

The sediments of Unit C are clay-rich and display weak internal stratification. Extrapolation across the cave-chamber,

Fig. 2.17 Photograph of the geological trench (Pit 3; see Fig. 2.16) excavated in the entranceway to Azokh 5. Two units (1 and 2) are clearly visible. The northeastern edge of the trench is indicated with a dashed black line. Hammer (circled) for scale

southwest towards the exit, indicates that when this horizon was being deposited the passage connecting to the outside may have been sealed. Unit C most likely was produced by very quiet conditions (still-water deposition), and, given its thickness of 26–34 cm, it may have taken an appreciable amount of time to form. Therefore, although Unit A may be (perhaps late) Holocene in age, with the discordant relationship with underlying Unit B and the potential amount of time required to deposit Unit C, it is possible that Units D and E below may be significantly older.

Discussion on the Stratigraphy of Azokh 5

At present, it is unclear precisely how the two sedimentary sections (external and internal) in Azokh 5 physically and temporally relate to one another. A simple topographic assessment suggests that Units A–E in the inner chamber may overlie Units 2–3 located closer to the cave entrance (see Fig. 2.16); however, this requires more excavation work to unequivocally confirm or disprove this relationship. A further complication is that natural fracturing and

Fig. 2.18 Photomontage of the sediment section present inside Azokh ► 5 inner chamber. The five units (A–E) are marked in the photo and the tape measure scale is extended to 318 cm

Table 2.4 Stratigraphy of Azokh 5 inner chamber

Unit	Thickness	Consistence & Texture	Structure	Color (Munsell)	Rocks/clasts/comments	Carbonates
A	200 cm+ (*Minimum value – unit thickens considerably in direction of cave interior; top not seen*)	Friable-firm clay	Fine granular to massive	10YR 6/4 (Light yellowish brown)	Limestone clasts are very rare. This unit is well sorted and stratified (laminated) and drapes the irregular surface topography of Unit B below	Strongly Calcareous
B	c. 55–85 cm+ (*Thins to c. 34 cm in NW corner of chamber, appears to be thickest in SE corner*)	Friable silty clay	Medium granular	7.5YR 5/4 (Brown)	Highly mixed and unsorted unit. Varies between essentially a matrix- and clast-supported breccia. Contains abundant limestone clasts (on all scales). Chert clasts noted also	Non-calcareous
C	26–34 cm	Friable clay (*Very firm when dry*)	Largely massive	7.5YR 4/2.5 (Brown)	Clasts generally rare: granule and pebble-scale clasts of limestone and angular chert present but not conspicuous. Unit has some weak internal stratification. Drapes irregular topography of Unit D below; basal contact is sharp	Non-calcareous
D	64–66 cm	Friable sandy clay	Medium granular	7.5YR 4.5/3 (Brown)	Matrix-supported breccia. Clasts of all sizes, although 2–7 mm whitish granules and pebbles are most conspicuous. Larger clasts (up to 13 cm across) are generally located in the upper half of the unit. Clasts consist of limestone (displaying varying degrees of decalcification) and angular dark clasts of chert (up to 7.5 cm)	Non-calcareous
E	90 cm (*Minimum – base not seen*)	Friable (to loose) sandy clay	Medium granular	7.5YR 5/3 (Brown)	Moderately well sorted unit, although rare 1–3 mm granules are present. Basal 50–60 cm has a vague horizontal internal stratification developed. Thin white non-calcareous crust (3–5 mm) caps unit in northern corner of cave chamber	Non-calcareous

Fig. 2.19 Flattened cylindrical structure, possibly a calcified mammal burrow, from the inner chamber of Azokh 5

displacement of Units A–E has been observed in the inner chamber. It appears that these units have begun to slip progressively downwards in the direction of the cave exit (Fig. 2.16). In addition, Domínguez-Alonso et al. (2016) note that geophysical investigations have indicated over 10 m (stratigraphic thickness) of sediments infilling Azokh 5. Thus, further investigation of the passage is likely required to improve our understanding of the sediments within Azokh 5.

Conclusions

1. Of the three passages connecting to the interior of the Azokh Cave system, the stratigraphy of Azokh 1, previously documented in detail by Murray et al. (2010), is the most completely known. This particular passage has been excavated since the 1960s and contains an 11–12 m thick sedimentary record dating from at least the Middle Pleistocene (and possibly even older; see Table 2.1) to the present. The Pleistocene-Holocene transition is not seen due to a marked erosional disconformity in the sequence towards the very top.
2. A lower-lying sub-chamber in the Azokh 1 Passage (see Fig. 2.4), close to the entrance, accommodates Sediment Sequence 1. This 4.5 m thick section includes Units IX to VI (in ascending stratigraphic order), and, with the

exception of the very top, it is apparently largely unfossiliferous. For this reason, the precise age of these sediments remains unknown. Previous paleomagnetic work suggested that the base of the succession, in this part of the cave, might in fact be Early Pleistocene in age.

3. Sediment Sequence 2 is located further in from the cave entrance in Azokh 1 and is interpreted to have largely overlain Sediment Sequence 1, although this is not possible to verify as they are no longer physically connected due to past excavation work. This sequence is about 8.5 m thick and is divisible into five units (V–I). The lowermost Unit V accounts for almost half this thickness estimate. Units V–II have produced a rich and diverse Middle to Upper Pleistocene fauna. Associated and isolated cave bear skeletal and dental elements are particularly conspicuous throughout this part of the succession. Evidence of human activity (in the form of stone tools and cut marks on bones) has also been found in these levels. In the past, a Middle Pleistocene human mandible fragment was recovered from about the level of Unit V, although the precise datum of this find is unclear.
4. The sedimentary infill of the Azokh 1 passage is generally fine-grained, suggesting either very low energy water-flow, perhaps due to ponding as a result of flooding further inside the cave system, or due to possible wind-blown deposition, although this is unlikely for sediments located further inside from the cave entrance. Horizons containing concentrations of coarser limestone debris also occur. Their significance is unclear; however, they may indicate a change in paleoenvironmental conditions, such as an increase in water percolation through the cave or a marked climatic cooling. Geomorphological and tectonic factors, such as an increase in earthquake activity, cannot be discounted either.
5. Azokh 2 is a smaller cave located 42 m NNW from the entrance to Azokh 1. At present two stratigraphic units are clearly identifiable infilling the passage. The uppermost of these (Unit 1) appears to be Holocene in age and below this, Unit 2 is conspicuously lighter in color and more calcareous. Its total thickness is unproven and, as it did not produce any fossils or artifacts, its age is unknown. A significant boulder collapse in the rear of Azokh 2 continues to pose serious logistical problems for further excavation of the cave passage.
6. Azokh 5 is located 100 m NNW from Azokh 1. It is a small phreatic tube that leads to an inner chamber containing at least 4.5 m of infill, although that value is likely to be a gross underestimate as the base and top of the sequence were not seen and geophysical results reported by Domínguez-Alonso et al. (2016) suggests a total sediment infill of at least 10 m. At present five units (labeled A–E in descending stratigraphic order) have been identified. The sediments are generally fine-grained, although Units D and B both contain elevated amounts of coarse limestone and chert debris, much of which has been locally sourced. A disconformable relationship has been identified between Units B and A at the very top of the succession. Unit A has produced charcoal dating to c. 2,300 years BP (Fernández-Jalvo et al. 2010); however, the age of the units beneath remains unknown at present.

Spectroscopy Methodology

Raman Spectroscopy of Azokh 1 Sediment Samples: Analytical Methodology

Raman spectroscopy of sediment samples was conducted at the School of Natural Sciences, NUI Galway, using a Horiba LabRam HR laser Raman spectrometer. The instrument is equipped with a 600 groove.mm^{-1} diffraction grating, confocal optics and a Peltier-cooled CCD detector (255 × 1024 pixel array at −67 °C) coupled to an Olympus BX51 microscope. Dry, friable samples were placed on a glass slide and analysed in 180° backscatter mode using either 532 nm or 784 nm laser excitation channeled through a 50× microscope objective. Individual analyses were performed for between 60–90 s over the spectral range 100–1800 cm^{-1} (Fig. 2.14). The number of spectral accumulations per analysis typically ranged between 50 and 100 in order to maximize the signal-to-noise efficiency of the spectrometer. Calibration of the instrument was routinely performed between analyses using the Raman peak of a crystalline silicon wafer (520.2 ± 0.5 cm^{-1}; Parker et al. 1967). Spectral uncertainty associated with the generation of Raman peak positions is estimated to be ±1.5 cm^{-1} (2σ) under 532 nm laser excitation and ±1.0 cm^{-1} (2σ) using the 783 nm laser.

Acknowledgments Many colleagues have helped and offered much valuable advice to us on numerous aspects of the stratigraphy and sedimentology over the years. In particular, we wish to sincerely thank Yolanda Fernández-Jalvo, Peter Andrews and Peter Ditchfield for very generously sharing their expertise, knowledge and opinions. Teresa Sanz Martín supplied some of the photographs used in the figures. The Royal Irish Academy is thanked for kindly granting permission to reproduce several figures from Murray et al. (2010). The help and assistance of the local people at the excavation at Azokh, year after year, is much appreciated. Without their input, the Azokh Project simply could not run.

References

Appendix: Fernández-Jalvo, Y., Ditchfield, P., Grün, R., Lees, W., Aubert, M., Torres, T., et al. (2016). Dating methods applied to Azokh cave sites. In Y. Fernández-Jalvo, T. King, L. Yepiskoposyan & P. Andrews (Eds.), *Azokh Cave and the Transcaucasian Corridor* (pp. 321–339). Dordrecht: Springer.

Asryan, L., Moloney, N., & Ollé, M. (2016). Lithic assemblages recovered from Azokh 1. In Y. Fernández-Jalvo, T. King, L. Yepiskoposyan & P. Andrews (Eds.), *Azokh Cave and the Transcaucasian Corridor* (pp. 85–101). Dordrecht: Springer.

Bogli, A. (1980). *Karst hydrology and physical speleology*. Berlin: Springer.

Bretz, J. H. (1942). Vadose and phreatic features of limestone caverns. *Journal of Geology, 50*, 675–811.

Bridgland, D. R., Antoine, P., Limondin-Lozouet, N., Santisteban, J. I., Westaway, R., & White, M. J. (2006). The Palaeolithic occupation of Europe as revealed by evidence from the rivers: Data from IGCP 449. *Journal of Quaternary Science*, *21*, 437–455.

Chauvet, J.-M., Deschamps, E. B., & Hillaire, C. (1996). *Dawn of art: The Chauvet Cave*. New York: Harry N. Abrams.

Dirks, P. H. G. M., Kibii, J. M., Kuhn, B. F., Steininger, C., Churchill, S. E., Kramers, J. D., et al. (2010). Geological Setting and Age of *Australopithecus sediba* from Southern Africa. *Science, 328*, 205–208.

Domínguez-Alonso, P., Aracil, E., Porres, J. A., Andrews, P., Lynch E. P. & Murray, J. (2016). Geology and geomorphology of Azokh Caves. In Y. Fernández-Jalvo, T. King, L. Yepiskoposyan & P. Andrews (Eds.), *Azokh Cave and the Transcaucasian Corridor* (pp. 55–84). Dordrecht: Springer.

Doronichev, V. B. (2008). The Lower Paleolithic in Eastern Europe and the Caucasus: A reappraisal of the data and new approaches. *PaleoAnthropology*, 107–157.

Doronichev, V., & Golonova, L. (2010). Beyond the Acheulean: A view on the Lower Palaeolithic occupation of Western Eurasia. *Quaternary International, 223–224*, 327–344.

Engel, A. S., Stern, L. A., & Bennett, P. C. (2004). Microbial contributions to cave formation: New insights into sulfuric acid speleogenesis. *Geology, 32*, 369–372.

Fernández-Jalvo, Y., Hovsepian-King, T., Moloney, N., Yepisko posyan, L., Andrews, P., Murray, J., et al. (2009). *Azokh Cave project excavations 2002–2006: Middle-Upper Palaeolithic transition in Nagorno-Karabagh*. Coloquios de Paleontología, Special Issue: Homage to Dr. D. Soria Madrid, Universidad Complutense de Madrid Press.

Fernández-Jalvo, Y., King, T., Andrews, P., Yepiskoposyan, L., Moloney, N., Murray, J., et al. (2010). The Azokh Caves complex: Middle Pleistocene to Holocene human occupation in the Caucasus. *Journal of Human Evolution, 58*, 103–109.

Fernández-Jalvo, Y., King, T., Andrews, P., & Yepiskoposyan, L. (2016). Introduction: Azokh Cave and the Transcaucasian Corridor. In Y. Fernández-Jalvo, T. King, L. Yepiskoposyan & P. Andrews (Eds.), *Azokh Cave and the Transcaucasian Corridor* (pp. 1–26). Dordrecht: Springer.

Ford, D. C., & Williams, P. (2007). *Karst Hydrogeology and Geomorphology*. Chichester: Wiley.

Huseinov, M. M. (1985). *The Early Palaeolithic of Azerbaijan (Kuruchai culture and stages of its development).* Baku (in Russian).

Jelinek, A. J. (1982). The Tabun Cave and Paleolithic Man in the Levant. *Science, 216*, 1369–1375.

Karkanas, P., Bar-Yosef, O., Goldberg, P., & Weiner, S. (2000). Diagenesis in Prehistoric Caves: The Use of Minerals that Form *In Situ* to Assess the Completeness of the Archaeological Record. *Journal of Archaeological Science, 27*, 915–929.

Karkanas, P., Rigaud, J.-P., Simek, J., Albert, R., & Weiner, S. (2002). Ash, bones and guano: A study of the minerals and phytoliths in the sediments of Grotte XVI, Dordogne, France. *Journal of Archaeological Science, 29*, 721–732.

Kasimova, R. M. (2001). Anthropological research of Azykh Man osseous remains. *Human Evolution, 16*, 37–44.

Khain, V. E. (1997). Azerbaijan. In E. M. Moores & R. W. Fairbridge (Eds.), *Encylcopedia of European and Asian regional geology*. London: Chapman & Hall.

King, T., Compton, T., Rosas, A., Andrews, P. Yepiskoyan, L., & Asryan, L. (2016). Azokh Cave Hominin Remains. In Y. Fernández-Jalvo, T. King, L. Yepiskoposyan & P. Andrews (Eds.), *Azokh Cave and the Transcaucasian Corridor* (pp. 103–106). Dordrecht: Springer.

Kizewski, F., Liu, Y. T., Morris, A., & Hesterberg, D. (2011). Spectroscopic approaches for phosphorus speciation in soils and other environmental systems. *Journal of Environmental Quality, 40*, 751–766.

Lioubine, V. P. (2002). *L'Acheuléen du Caucuase*. ERAUL 93 Études et Recherches Archéologiques de l'Université de Liège. Liège.

Ljubin, V. P., & Bosinski, G. (1995). The earliest occupation of the Caucasus region. In W. Roebroeks & T. van Kolfschoten (Eds.), *The Earliest Occupation of Europe* (pp. 207–253). Leiden: University of Leiden.

Magela da Costa, G., & Rúbia Ribeiro, V. (2001). The occurrence of tinsleyite in the archaeological site of Santana do Riacho, Brazil. *American Mineralogist, 86*, 1053–1056.

Marin-Monfort, M. D., Caceres, I., Andrews, P., Pinto A. C. & Fernández-Jalvo, Y. (2016). Taphonomy and Site Formation of Azokh 1. In Y. Fernández-Jalvo, T. King, L. Yepiskoposyan & P. Andrews (Eds.), *Azokh Cave and the Transcaucasian Corridor* (pp. 211–249). Dordrecht: Springer.

Marincea, S., Dumitras, D., & Gibert, R. (2002). Tinsleyite in the "dry" Cioclovina Cave (Sureanu Mountains, Romania): The second occurrence. *European Journal of Mineralogy, 14*, 157–164.

Moldovan, O. T., Mihevc, A., Mikó, L., Constantin, S., Meleg, I., Petculescu, A., et al. (2011). Invertebrate fossils from cave sediments: A new proxy for pre-Quaternary paleoenvironments. *Biogeosciences, 8*, 1825–1837.

Moore, G. W., & Sullivan, N. (1997). *Speleology: Caves and the cave environment*. St. Louis: Cave Books.

Murray, J., Domínguez-Alonso, P., Fernández-Jalvo, Y., King, T., Lynch, E. P., Andrews, P., et al. (2010). Pleistocene to Holocene stratigraphy of Azokh 1 Cave, Lesser Caucasus. *Irish Journal of Earth Sciences, 28*, 75–91.

Musgrave, R. J. & Webb, J. A. (2004). Palaeomagnetic analysis of Sediments on the Buchan Caves, Southeastern Australia, Provides a Pre-Late Pleistocene Date for Landscape and Climate Evolution. In I. D. Sasowsky & J. E. Mylroie (Eds.), *Studies of Cave Sediments. Physical and Chemical Records of Paleoclimate*. Dordrecht: Springer/Kluwer Academic Publisher.

Mustafayev, A. (1996). Jawbones and Dragon Legends. *Azerbaijan's Prehistoric Azikh Cave. Azerbaijan International, 4*(2), 24–32.

Parker, J. H., Feldman, D. W., & Ashkin, M. (1967). Raman Scattering by silicon and germanium. *Physical Review, 155*(3), 712–714.

Pickering, R., Hancox, P. J., Lee-Thorp, J. A., Grün, R., Mortimer, G. E., McCulloch, M., et al. (2007). Stratigraphy, U-Th chronology, and paleoenvironments at Gladysvale Cave: Insights into the climatic control of South African hominin-bearing cave deposits. *Journal of Human Evolution, 53*, 602–619.

Pickering, R., Kramers, J. D., de Hancox, P. J., Ruitere, D. J., & Woodhead, J. D. (2011). Contemporary flowstone development links early hominin bearing cave deposits in South Africa. *Earth and Planetary Science Letters, 306*, 23–32.

Pinhasi, R., Gasparian, B., Wilkinson, K., Bailey, R., Bar-Oz, G., Bruch, A., et al. (2008). Hovk 1 and the Middle and Upper Paleolithic of Armenia: A preliminary framework. *Journal of Human Evolution, 55*, 803–816.

Pinhasi, R., Gasparian, B., Nahapetyan, S., Bar-Oz, G., Weissbrod, L., Bruch, A. A., et al. (2011). Middle Palaeolithic human occupation of the high altitude region of Hovk-1, Armenia. *Quaternary Science Reviews, 30*, 3846–3857.

Polyak, V. J., McIntosh, W. C., Güven, N., & Provencio, P. (1998). Age and origin of Carlsbad Cavern and related caves from $^{40}Ar/^{39}Ar$ of alunite. *Science, 279*, 1919–1922.

Sasowsky, I. D., & Mylroie, J. E. (2004). *Studies of Cave Sediments. Physical and Chemical Records of Paleoclimate*. Dordrecht: Springer/Kluwer Academic Publisher.

Sevilla, P. (2016). Bats from Azokh Caves. In Y. Fernández-Jalvo, T. King, L. Yepiskoposyan & P. Andrews (Eds.), *Azokh Cave* *and the Transcaucasian Corridor* (pp. 177–189). Dordrecht: Springer.

Shahack-Gross, R., Berna, F., Karkanas, P., & Weiner, S. (2004). Bat guano and preservation of archaeological remains in cave sites. *Journal of Archaeological Science, 31*, 1259–1272.

Sinyayev, V. A., Shustikova, E. S., Griggs, D., & Dorofeev, D. V. (2005). The nature of P–O bonds in the precipitated amorphous calcium phosphates and calcium magnesium phosphates. *Glass Physics and Chemistry, 31*, 671–675.

Smith, C. I., Faraldos, M., & Fernández-Jalvo Y. (2016). Bone Diagenesis at Azokh Caves. In Y. Fernández-Jalvo, T. King, L. Yepiskoposyan & P. Andrews (Eds.), *Azokh Cave and the Transcaucasian Corridor* (pp. 251–269). Dordrecht: Springer.

Torres, T., Ortiz, J. E., & Cobo, R. (2003). Features of Deep Cave Sediments: Their Influence on Fossil Preservation. *Estudios Geológicos, 59*, 195–204.

Van der Made, J., Torres, T., Ortiz, J. E., Moreno-Pérez, L., & Fernández-Jalvo, Y. (2016). The new material of large mammals from Azokh and comments on the older collections. In Y. Fernández-Jalvo, T. King, L. Yepiskoposyan & P. Andrews (Eds.), *Azokh Cave and the Transcaucasian Corridor* (pp. 117–159). Dordrecht: Springer.

White, W. B. (1988). *Geomorphology and hydrology of karst terrains*. New York: Oxford University Press.

White, W. B. (2007). Cave sediments and paleoclimate. *Journal of Cave and Karst Studies, 69*, 76–93.

http://www.springer.com/978-3-319-24922-3

Azokh Cave and the Transcaucasian Corridor
Fernández-Jalvo, Y.; King, T.; Yepiskoposyan, L.; Andrews, P. (Eds.)
2016, XVII, 349 p. 174 illus., 67 illus. in color., Hardcover
ISBN: 978-3-319-24922-3